REPORT NO.
NADC-81087-60

LEVEL II

Approved for Public Release;
Distribution Unlimited

A Review of Advanced Acoustic Emission Sensors

D. K. Lemon

April 1981

Prepared for
Naval Air Development Center
Warminster, Pennsylvania
under Contract N62269-80-C-0243

Sponsor: Defense Advanced Research
Projects Agency
DARPA Order No. 3905

Battelle
Pacific Northwest Laboratories

Unclassified

SECURITY CLASSIFICATION OF THIS PAGE (When Data Entered)

REPORT DOCUMENTATION PAGE

READ INSTRUCTIONS BEFORE COMPLETING FORM

1. REPORT NUMBER: NADC-81087-60	2. GOVT ACCESSION NO.: AD-A098989
3. RECIPIENT'S CATALOG NUMBER:	
4. TITLE (and Subtitle): A Review of Advanced Acoustic Emission Sensors	5. TYPE OF REPORT & PERIOD COVERED: Interim rept.,
6. PERFORMING ORG. REPORT NUMBER: 23111-04210	
7. AUTHOR(s): D. K. Lemon	8. CONTRACT OR GRANT NUMBER(s): N62269-80-C-0243, AMD // DARPA Order-3905
9. PERFORMING ORGANIZATION NAME AND ADDRESS: Battelle, Pacific Northwest Laboratories, P.O. Box 999, Richland, WA 99352	10. PROGRAM ELEMENT, PROJECT, TASK AREA & WORK UNIT NUMBERS: 134
11. CONTROLLING OFFICE NAME AND ADDRESS: Defense Advanced Research Projects Agency, 1400 Wilson Boulevard, Arlington, VA 22209	12. REPORT DATE: April 1981
	13. NUMBER OF PAGES: 157
14. MONITORING AGENCY NAME & ADDRESS (if different from Controlling Office): Naval Air Development Center, Street and Jacksonville Roads, Warminster, PA 18974	15. SECURITY CLASS. (of this report): Unclassified
	15a. DECLASSIFICATION/DOWNGRADING SCHEDULE:

16. DISTRIBUTION STATEMENT (of this Report)

Approved for Public Release; Distribution Unlimited

17. DISTRIBUTION STATEMENT (of the abstract entered in Block 20, if different from Report)

18. SUPPLEMENTARY NOTES

None

19. KEY WORDS (Continue on reverse side if necessary and identify by block number)

Acoustic Emission, Advanced Sensors, Broadband Piezoelectric, Nondestructive Testing

20. ABSTRACT (Continue on reverse side if necessary and identify by block number)

This report describes work done to evaluate emerging, advanced sensors for detection of acoustic emission from fatigue crack growth. The task reported herein is part of an overall project whose objective is to develop acoustic emission monitoring of fatigue crack growth in aircraft. In Section 1, the operation of each candidate sensor is summarized. Section 2 describes the criteria used to evaluate the suitability of each sensor for

over

DD FORM 1 JAN 73 1473 EDITION OF 1 NOV 65 IS OBSOLETE S/N 0102-LF-014-6601

Unclassified

SECURITY CLASSIFICATION OF THIS PAGE (When Data Entered)

401048

JOB

(cont)

near-term use on this acoustic emission project. ~~In Section 3, we present our~~ recommendations regarding which sensor concepts appear to be most promising within the context of the project's needs. The appendices ~~to this report~~ contain papers that were submitted to Battelle by various experts discussing the sensor concepts.

Accession For	
NTIS GRA&I	☑
DTIC TAB	☐
Unannounced	☐
Justification	
By	
Distribution/	
Availability Codes	
Dist	Avail and/or Special
A	

TOPICAL REPORT

A REVIEW OF ADVANCED ACOUSTIC EMISSION SENSORS

D.K. LEMON

March 1981

Prepared for
Naval Air Development Center
Warminster, Pennsylvania
under project 23111 04210

Battelle
Pacific Northwest Laboratories
Richland, Washington 99352

TOPICAL REPORT

ARPA ORDER NO.: 3905 PROGRAM CODE NO.: 0Y10

CONTRACTOR: Battelle
Pacific Northwest Laboratories

CONTRACT NO.: N62269-80-C-0243

EFFECTIVE DATE OF CONTRACT: May 29, 1980

EXPIRATION DATE OF CONTRACT: November 29, 1982

PRINCIPAL INVESTIGATOR: P.H. Hutton

TELEPHONE NO.: (509) 375-2157

SHORT TITLE OF WORK: Acoustic Emission Monitoring of Aircraft to Detect Fatigue Crack Growth

ACKNOWLEDGEMENTS

The work reported herein is part of a project monitored by Dr. Michael Buckley of the Defense Advanced Research Projects Agency (DARPA) and Mr. John Carlyle of the Naval Air Development Center (NADC). We appreciate their guidance and input throughout the course of the evaluation of AE sensor concepts.

Several individuals contributed papers to Battelle reviewing specific sensor concepts. With their permission, these papers are included in the appendices of this report. We acknowledge these contributions by L. J. Busse, Battelle Northwest; W. A. Schulze, Pennsylvania State University; B. Thompson, Ames Laboratory; R. M. White, University of California-Berkeley; T. Proctor, National Bureau of Standards; D. Eitzen, National Bureau of Standards, W. R. Scott, Naval Air Development Center, and G. Kino, Stanford University. We also benefited from discussions with Pierre Khuri-Yakub of Stanford University, as well as with J. Bucaro and J. Cole from the Naval Research Laboratory.

ABSTRACT

This report describes work done to evaluate emerging, advanced sensors for detection of acoustic emission from fatigue crack growth. The task reported herein is part of an overall project whose objective is to develop acoustic emission monitoring of fatigue crack growth in aircraft. In Section 1, the operation of each candidate sensor is summarized. Section 2 describes the criteria used to evaluate the suitability of each sensor for near-term use on this acoustic emission project. In Section 3, we present our recommendations regarding which sensor concepts appear to be most promising within the context of the project's needs. The appendices to this report contain papers that were submitted to Battelle by various experts discussing the sensor concepts.

TABLE OF CONTENTS

SUMMARY

The task reported herein is part of a program to develop acoustic emission monitoring of aircraft to detect fatigue crack growth. The program's technical approach is based on pattern recognition methods for distinguishing crack-related acoustic emission from interfering, ofter similar, acoustic energy in the specimen. The ability to make such distinctions is especially important in aircraft because of the fretting noise generated by the many rivets and bolts.

The pattern recognition technique utilizes the spectral content of the AE waveforms. Therefore, the transfer function or bandwidth of the AE sensor is important to the success of the technique. For this reason, the "Sensor Evaluation Task" described in this report was established. The goal of this task is to evaluate emerging, advanced sensor concepts that offer improved operating characteristics. The end result of this task is a recommendation regarding those sensors that appear to be most promising in context of the program's technical needs and time schedule.

The sensors were evaluated based on both technical and practical criteria. The technical criteria are bandwidth, sensitivity, phase uniformity, fidelity of response, element size, capacitance and directionality. The practical criteria are availability of the sensor for near term use, the sensor's present state of development, and the projected feasibility of implementing the concept in a field-usable form.

After evaluating each sensor in terms of these criteria, we recommend that two sensors be explored for further development. They are the point-displacement sensor and broadband piezoelectric sensors. These recommendations are consistent with the independent conclusions given in the paper by Gordon Kino (Appendix G). Both of these sensor types promise to provide improved operating characteristics and yet be available within the necessary time frame.

A REVIEW OF ADVANCED ACOUSTIC EMISSION SENSORS

D. K. Lemon

INTRODUCTION

One promising application of acoustic emission (AE) technology is for in-flight monitoring of fatigue crack growth in critical aircraft components. One of the challenges of this application is the presence of competing acoustic noise in the structure beside the time crack-related AE. Furthermore, noise from the fretting of fasteners occurs at the same location as the cracks. Hence, simple spatial location of emission is not sufficient to determine if crack growth is occurring. The project under which this task was performed addresses the problem of distinguishing crack-related AE from other acoustic energy that is present in a test specimen. This discrimination is being done through computerized pattern recognition analysis of digitized AE waveforms. The AE waveforms are generated through actual fatigue tests of materials encountered in aircraft structures.

The pattern recognition analysis relies heavily upon the frequency content of the AE waveforms. Hence, the transfer function or bandwidth of the AE sensors is of prime importance. For this reason, a task was established to review emerging, advanced AE sensor concepts with the objective of ultimately providing improved sensors for use on this project.

A list of cnadidate sensors was developed and review of papers were solicited from persons expert on each particular sensor concept. The sensors considered are the acousto-electric receiver, broadband piezoelectric sensors, composite piezoelectrics, electromagnetic transducers, fiber-optic sensors, a ZnO-FET transducer, a point-displacement sensor and sensors made of PVF film. In addition, a paper was submitted by Gordon Kino giving an independent review of these sensors.

It should be emphasized that the criteria used in evaluating the candidate sensors were selected based on the technical needs and time schedule of this project. Consequently, the recommendations given herein are not necessarily an indication of the ultimate potential of a sensor, given different technical requirements or time and funds.

The three sections that follow cover (1) the sensor concepts considered, (2) the evaluation criteria, and (3) recommendations.

The sensor development task itself consists of three phases:

A. Preparation of review papers on advanced sensor concepts written by experts on each topic. Section 1 summarizes each concept; the contributed papers are contained in the appendices.

B. Evaluation of the advanced concepts. Section 2 describes the criteria used to evaluate the sensor concepts.

C. Development of working models of one or two sensor designs. Section 3 presents our recommendations regarding those sensors that appear to be most beneficial to the AE - NADC project.

SECTION 1: THE SENSOR CONCEPTS

To accomplish Phase A of the Sensor Development Task, Battelle solicited papers from individuals, each of whom is an expert on a particular sensor concept. Table 1 lists the concepts considered and contributing consultants. The entire texts of the contributed papers are enclosed in the appendices of this report.

Table I

Advanced AE Sensors
Topic and Contributor

Sensor Concepts	Contributing Consultants
Acousto-Electric	L.J. Busse, Battelle Northwest
Broadband Piezoelectrics*	L.J. Busse, Battelle Northwest Pierre Kuri Jacob, Stanford University
Composite Piezoelectrics	W.A. Schulze, Pennsylvania State University
EMAT's	B. Thompson, Ames Laboratory
Fiber-Optic*	J. Carlyle, NADC D.K. Lemon, Battelle Northwest
FET-ZnO	R.M. White, University of California-Berkeley
NBS Point Displacement Sensor	T. Proctor and D. Eitzen, National Bureau of Standards
PVF Film	W.R. Scott, Naval Air Development Center
General Review of All Concepts	G. Kino, Stanford University

*These concepts were evaluated based on personal communications from the consultants shown. Consequently, no papers appear in the appendices for these concepts.

A brief description of each concept is given below:

- Acousto-electric receiver: This receiver is based on the acousto-electric effect of a cadmium sulfide crystal which is a piezoelectric semiconductor. As a stress wave propagates through the crystal, a net flow of charge is produced. The

resulting voltage is proportional to the intensity of the incoming wave and insensitive to the phase.

- Broadband piezoelectric transducers: This refers to sensors having conventional piezoelectric elements that have been designed for maximum bandwidth. Through modelling of the electrical and mechanical parameters, the bandwidth of AE-type sensors can be estimated. Mechanical and electrical matching considerations are an integral part of the design and fabrication procedure.

- Composite piezoelectric sensors: The composite material consists of PZT material embedded in a polymer matrix. The simplest form of the composite consists of parallel rods of PZT in a polymer binder. By varying the length of the rods (and hence their natural resonances) the bandwidth of the sensor can be adjusted.

- EMAT or electromagnetic acoustic transducer: The EMAT utilizes electromagnetic forces to detect ultrasonic vibrations in conducting materials. The sensor consists of a coil of wire and a magnet. By adjusting the coil and the orientation of the magnetic field, the sensor can be made to respond to shear or longitudinal waves.

- Fiber optic sensors: Recent investigations[1,2,3] have shown a fiber optic interferometer to be a sensitive and versatile hydrophone. The fiber optic detector is one "leg" of an interferometer. A passing sound wave causes an increased optical path length in the fiber due to changes in its index of refraction and length. Hence, there is a phase modulation in the reconstructed light beam proportional to the sound wave input. The state-of-the-art is advancing rapidly with small, integrated components being developed rapidly. At present, fiber optic sensing systems are set up with discrete components on an optical table. As the technology progresses, small, self-contained systems may become available.

- ZnO-FET transducers: The active element of this transducer is a thin film of zinc-oxide (ZnO) that is deposited on a silicone substrate. A field effect transistor is also formed integrally on the substrate. The transduction occurs when the voltage developed by the ZnO film acts on the FET. The output of the FET is therefore a function of the sound wave input.

- The NBS point displacement transducer: This transducer uses a conical piezoelectric element. With present models, the tip of the core is in direct contact with the test specimen, hence a point-like contact is obtained. The sensor responds to the vertical component of the test surface motion.

- The PVF film transducer: This transducer is based on the piezoelectric properties of PVF film. Since the film is thin, there are no resonances in the frequency range of interest in AE.

SECTION 2: EVALUATION CRITERIA

During Phase B of the task, the sensor concepts were reviewed and evaluated based on both technical and practical criteria. The evaluation criteria are given in Table II.

Table II
Evaluation Criteria

Technical	Practical
Bandwidth-Sensitivity	Availability for near-term use
Phase uniformity	Present state of development
Fiedelity of response	Ability to be deployed in the field
Element size	
Capacitance	
Directionality	

These evaluation criteria are explained below:

TECHNICAL CRITERIA

- Bandwidth-sensitivity: The bandwidth of interest is 0.1 to 2.0 MHz (with greater emphasis on areas below 1 MHz). The optimum sensor would have a uniform bandwidth free from large nulls or drop-outs while maintaining sensitivity adequate to detect acoustic emissions.

- Phase Uniformity: This refers to the linearity or uniformity of the phase obtained from an FFT of a broadband input.

- Fidelity of Response: This term means the ability of the sensor to faithfully respond to a given input such as the veritcal component of displacement. The output from sensors that have a mixed response of longitudinal, radial or shear modes is difficult to

interpret quantitatively. Hence, a sensor with high "fidelity of response" is one whose output can be interpreted in terms of wave mode or surface displacement.

- Element size: The size of the sensing element is important in avoiding phase interference across the face of the sensor. To avoid such problems, the element diameter should be a wavelength or smaller.

- Capacitance: The capacitance of the sensor is important in driving the connecting cable. Because of the size constraint discussed above, some sensors do not have sufficient capacitance to adequately drive the connecting cable.

- Directionality: The directionality of the sensor refers to whether it is omni-directional or more sensitive in some directions. In some applications, an omni-directional sensor is desired. There are circumstances however where a directional sensor would be useful in filtering out noise sources.

PRACTICAL CRITERIA

- Availability for near-term use: Availability of the sensor for near-term use is necessary for the sensor to be of value to this current AE project. The objective of this sensor development task is to provide a sensor for use within the time frame of the project. Hence, near term availability is a necessity.

- Present state of development: The present state of development of a sensor concept is important because it influences the cost and risk involved in obtaining working models for project use. Whether the sensor is already available in the prototype stage or whether it is still in the concept stage are important practical considerations in selecting sensors for further evaluation.

- Ability to be deployed in the field: The sensors ultimately developed for this project should be able to function in the field. If a sensor is too fragile, too large, too temperature sensitive, etc., then field use will be restricted.

SECTION 3: RECOMMENDATIONS

Each of the candidate sensor concepts was evaluated based on the criteria discussed in Section 1. As a result of this evaluation, we recommend that two of the sensor concepts be explored further. The recommended concepts are:

1. The NBS Point Displacement Sensor: This sensor has an excellent combination of bandwidth, sensitivity and phase linearity. Its "fidelity of response" is also good because it responds only to the vertical motion of the test surface. The sensor is currently in the prototype stage, but laboratory models could be available within the time frame imposed by the project schedule. The aspect of development that remains to be addressed is adequate packaging of the sensor and a means for attaching it to a test specimen without degrading its performance.

2. Broadband Piezoelectric Sensors: Through application of advanced modelling and matching techniques[4,5] broadband piezoelectric sensors can be fabricated. Such sensors offer good bandwidth, sensitivity, size, and capacitance. We recommend that sensors of this type be further evaluated because of their promising characteristics.

At Battelle's request, a review paper of advanced AE sensors was prepared by Gordon Kino of Stanford University. His paper is given in entirety in Appendix G. In his paper, he eliminated many concepts because of low sensitivity or capacitance. He recommended use of a small disc of piezoelectric ceramic as the active element. His independent recommendation is consistent with the recommendation given above.

We conclude from this study of advanced AE sensors that there are sensors available in the near future that offer improved characteristics for recording AE waveforms. Such sensors would be positive to the AE program under which this task was undertaken.

REFERENCES

1. J. A. Bucaro, H. D. Dardy, and E. F. Carome, Appl. Opt. 16, 1761-1762 (L) (1977).

2. J. H. Cole, R. L. Johnson, and P. G. Bhuta, J. Acoust. Soc. Am. 62, 1136-1138 (1977).

3. H. L. Price, J. Acoust. Soc. Am. 66, 976-979 (1979).

4. C. S. Desilets, J. D. Fraser, and G. S. Kino, "The Design of Efficient Broad-Band Piezoelectric Transducers," IEEE SU-25, 115 (1978).

5. D. A. Leedom, R. Krimholtz, and G. L. Matthaie, "Equivalent Circuits for Transducers Having Arbitrary Even-or-Odd-Symmetry Piezoelectric Excitation," IEEE, SU-18, 128 (1971).

APPENDIX A

ADVANCED ACOUSTIC EMISSION SENSORS-- THE ACOUSTOELECTRIC RECEIVER

L. J. Busse
Battelle, Pacific Northwest Laboratories

ADVANCED ACOUSTIC EMISSION SENSORS--
THE ACOUSTOELECTRIC RECEIVER

L. J. Busse

PRESENT STATE OF TRANSDUCER CONCEPT

The acoustoelectric effect provides the physical basis for a phase insensitive ultrasonic receiving transducer known as the acoustoelectric receiver. The effect can be described as a classical wave particle drag phenomen. The waves involved are stress waves associated with the propagation of ultrasonic energy and the particles are conduction electrons which are free to move under the influence of an applied force. The acoustoelectric effect was first observed in n-type germanium,[1] however the most efficient acoustoelectric signal sources were soon found to be piezoelectric-semiconductors[2] in which the coupling of electrical and mechanical signals is directly facilitated. Cadmium sulfide has been the most commonly studied, acoustoelectrically active material because i) the piezoelectric effect is strong (CdS has higher electromechanical coupling than quartz),[2,3,4] ii) the semiconducting properties of CdS can be varied over many orders of magnitude (CdS is a photoconductor) and iii) large single crystals of CdS can be conveniently grown.[5,6]

As a stress wave propagates through a piezoelectric material, the spatially varying deformations lead to a spatially varying electric field distribution within the material. If this material is also a semiconductor (contains free charge carriers with density n_0 and finite mobility μ), these spatially varying electric fields will produce a spatially varying charge carrier distribution (bunching). When the time associated with charge "bunching" caused by the acoustic wave is comparable to the time associated with carrier "unbunching" due to Coulomb repulsion,

an irreversible transfer of energy between the acoustic and electronic system takes place. (When the ultrasonic frequency ω is approximately equal to the conductivity relaxation frequency, $\omega_c = \frac{\sigma}{\varepsilon}$, energy transfer is maximized.) In other words, the charge carriers will experience a force produced by the traveling stress wave. This force results in an observable current through the crystal (if short circuited) or a voltage across the crystal (if open circuited). This force can be described in terms of an effective electric field called the acoustoelectric field,

$$E_{AE}(\sigma,\omega) = \frac{-2\alpha_E(\sigma,\omega)}{N_o e v_s(\sigma,\omega)} \phi(\omega)$$

where α_E is the electronic attenuation coefficient, e is the electronic charge, v_s is the velocity of sound and ϕ is the instantaneous acoustic intensity. We see that the attenuation coefficient and the velocity of sound are both functions of the crystal conductivity σ; where $\sigma = n_o e \mu$. This equation, known as the Weinreich relation,[7] when integrated over the receiver length predicts the output caused by a particular acoustic mode or when integrated over frequency predicts the output caused by a broadband excitation.

The acoustoelectric receiver is a very broadband receiver in that it will produce an output over a wide range of ultrasonic frequencies. This broad frequency response is possible because the receiver is not a resonant device. For a fixed conductivity, the receiver output voltage has been observed[8] to be nearly constant over the frequency range of 2.5 to 9.5 MHz. This behavior is illustrated in Figure 1 where the receiver transfer function of the acoustoelectric receiver is compared with a conventional piezoelectric receiver for a constant incident intensity input of 0.5 watts/cm^2. By adjusting the conductivity, the acoustoelectric receiver has been used at higher frequencies as well.[9,10,11] As the operating frequency of the acoustoelectric receiver is lowered, however, so also must the conductivity of the detector be lowered. For practical size detectors the source impedance of the device will begin to exceed one megaohm at about one megahertz. For this reason, the

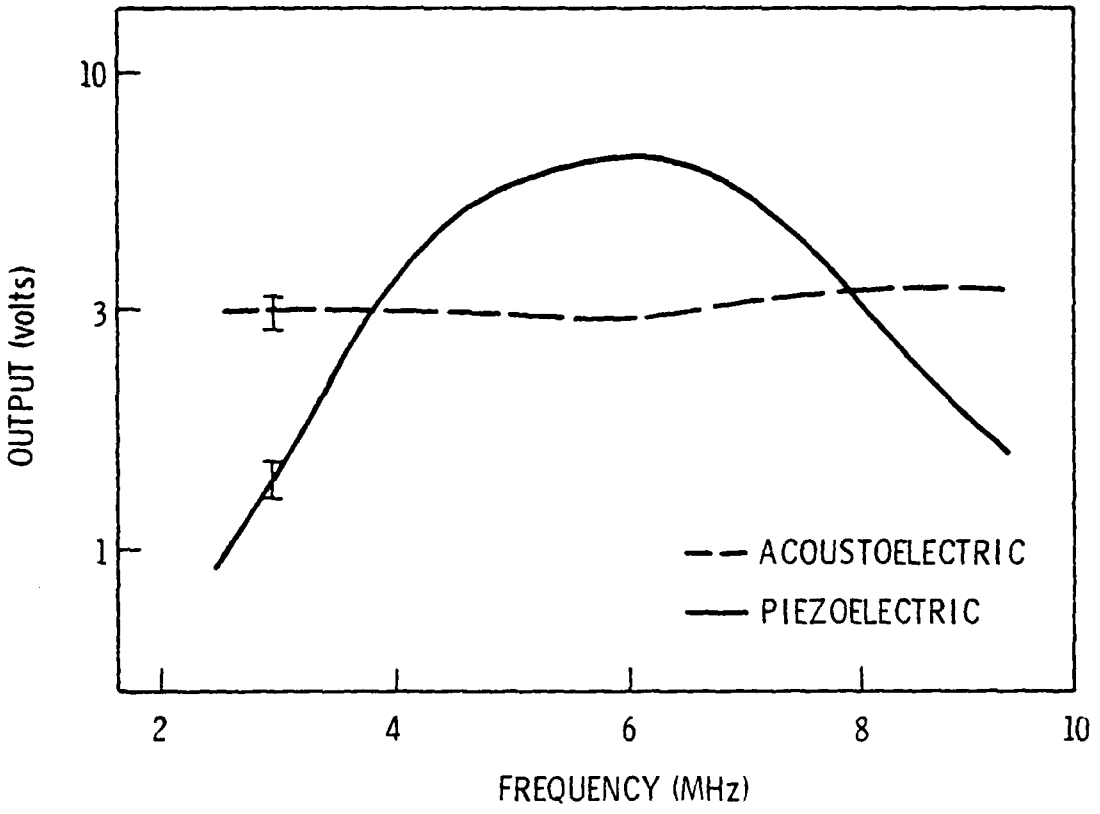

Figure 1. Broadband responsivity of the acoustoelectric voltage response of a CdS crystal. The acoustoelectric output in volts (dashed line) is shown for an instantaneous acoustic intensity input of 0.5 watt/cm^2 at each ultrasonic frequency measured. The responsivity of the acoustoelectric receiver is nearly frequency independent (varied by less than 1 dB) over the 2.5 to 9.5 MHz frequency range. The responsivity (solid line) of a commercially available broadband piezoelectric transducer over the same frequency range and for the same incident acoustic power level is shown for comparison.

practical application of an acoustoelectric receiver has not been demonstrated for ultrasonic frequencies below approximately 1 MHz.

It should be noted, that even though the receiver is a broadband device, the output of the device is not an RF voltage at the acoustic frequency. It is a DC or video signal whose time domain characteristics are determined by the temporal extent of the incident acoustic intensity and the

transit time through the detector.[9,10] Two pulses of equal intensity but different frequency will produce output voltages which are not distinguishable. For this reason, the acoustoelectric receiver may be best suited as an event detector or a total energy output monitor. Most of the frequency dependent measurements made using the acoustoelectric receiver were made when it was possible to control the frequency content of the incident pulse. Measurements have been made using swept tone bursts, chirped bursts, and broadband transient pulses under special conditions.[12]

The acoustoelectric receiver is a bulk wave device. Only waves which enter the receiver crystal and interact with the conduction electrons will be detected. Because the receiver relies upon piezoelectric coupling, the receiver is also somewhat mode selective. The bulk mode of interest must be piezoelectrically active. For example, in CdS, acoustoelectric receivers have been built for longitudinal wave detection (propagation parallel to the "c" crystalline axis) and for shear wave detection (propagation perpendicular to the "c" crystalline axis). In both of these cases the particle displacement associated with the acoustic disturbance is parallel to the "c" crystalline axis.

Acoustoelectric receivers are phase insensitive devices; i.e., they measure acoustic intensity not acoustic amplitude. As such, they have very broad beam characteristics or a broad acceptance angle. This point is demonstrated by Figure 2.[13] For equal aperture acoustoelectric and piezoelectric receivers, we see a much larger acceptance angle using the acoustoelectric receiver.

At present, acoustoelectric receivers are not commercially available. These devices have been fabricated by those involved in studying the basic phenomena and in applying the devices in measurement situations where phase insensitivity has been required.[9,13,14,15,16] These devices are therefore in a prototype state-of-development. The technology required for detector fabrication however requires relatively straightforward crystal orienting, cutting, and plating techniques.

A)

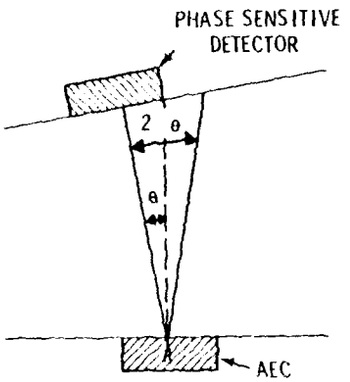

Figure 2A). Block Diagram of Variable Parallelism Water Cell.

B)

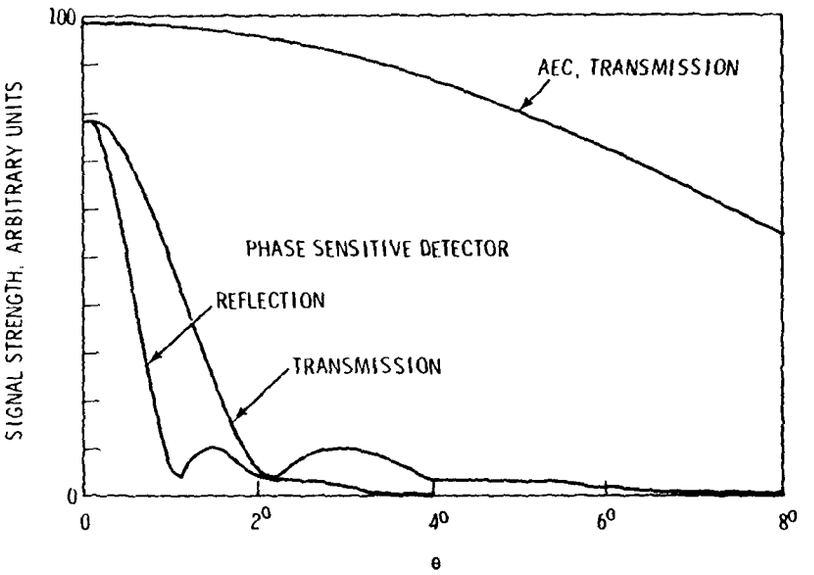

Figure 2B). Transducer Directivity Curves Obtained from Water Cell of Panel a.

DEVELOPMENT REQUIRED TO PROVIDE SEVERAL WORKING MODELS

The feasibility of detecting an acoustic emission event using an acoustoelectric receiver has not been demonstrated at this time. A successful demonstration of the device should take place before the cost involved in further development of a field model can be estimated. Sensitivity will be the biggest shortcoming of the acoustoelectric receiver. At present, the most sensitive devices operating at 5 MHz with bulk longitudinal waves have had a noise equivalent power of approximately one microwatt per square centimeter.[12] Comparable sensitivity (within a factor of three) to bulk shear waves can also be expected. As stated earlier, acoustoelectric receivers in their present form are not sensitive to surface waves.

The cost of fabricating an acoustoelectric receiver is approximately $1,500. Supporting electronics which would include video amplifiers, filters, and possibly a sample and hold unit could be assembled for approximately $500. Beyond this initial hardware investment, I would estimate that approximately one man-month would be necessary for transducer evaluation and an initial attempt at detecting an acoustic emission event.

REFERENCES

1. G. Weinreich, T. M. Sanders, Jr., and Harry G. White, "Acousto-electric Effect in *n*-Type Germanium," Phys. Rev. 114, 33-44 (1959).

2. Wen-Chung Wang, "Strong Acoustoelectric Effect in CdS," Phys. Rev. Letters 9, 443-445 (1962).

3. H. Gohecht and A. Bartschat, "Uber den Einfluss des Aktivators und der Speiherung von Strahlunepenergie aud das piezoelektrische und elastische verhalten von Cadmium sulfid-Einkristallen," Z. Physik 153, 529 (1959).

4. A. R. Hutson, "Piezoelectricity and Conductivity in ZnO and CdS," Phys. Rev. Letters 4, 505 (1960).

5. R. Frerichs, "The Photoconductivity of 'Incomplete Phosphors'," Phys. Rev. 72, 594 (1947).

6. D. R. Boyd and Y. T. Sihvones, "Vaporization - Crystalization Method for Growing CdS Single Crystals," J. Appl. Phys. 30, 176 (1959).

7. G. Weinreich, "Ultrasonic Attenuation by Free Carriers in Germanium," Phys. Rev. 107, 317 (1957).

8. L. J. Busse and J. G. Miller, "Broadband Acoustoelectric Receivers that Eliminate Phase Cancellation Effects," Proc. Third International Symposium on Ultrasonic Tissue Characterization, NBS (1978).

9. P. D. Southgate, "Use of a Power-Sensitive Detector in Pulse-Attenuation Measurements," J. Acoust. Soc. Am. 39, 480 (1966).

10. D. J. Larner, "The Acoustoelectric Voltage Generated in Cadmium Sulphide by a Narrow Input Acoustic Signal," Appl. Phys. Letters 15, 20.

11. V. E. Henrich and G. Weinreich, "Pulsed Ultrasonic Studies of the Acoustoelectric Effect, Ultrasonic Attenuation, and Trapping in CdS," Phys. Rev. 178, 1204 (1969).

12. L. J. Busse, "Electron-Phonon Interactions in Piezoelectric Semiconductors for the Phase Insensitive Detection of Ultrasound," Ph.D. Thesis, Washington University, St. Louis, MO (1979).

13. J. S. Heyman and J. H. Cantrell, "Application of Ultrasonic Phase Insensitive Receiver to Materials Measurements," 1977 Ultrasonics Symposium Proceedings, #77CH1264-1SU, 124.

14. L. J. Busse, J. G. Miller, D. Y. Yuhas, J. W. Mimbs, A. N. Weiss and B. E. Sobel, "Phase Cancellation Effects: A Source of Attenuation Artifact Eliminated by a CdS Acoustoelectric Receiver," Ultrasound in Medicine, Vol. 3, D. White, ed., (Plenum, New York, 1977), p. 1519.

15. J. S. Heyman, "Phase Insensitive Acoustoelectric Transducer," J. Acoust. Soc. Am. 64, 243 (1978).

16. J. R. Klepper, G. H. Brandenburger, L. J. Busse and J. G. Miller, "Phase Cancellation, Reflection and Refraction Effects in Quantitative Ultrasonic Attenuation Tomography," 1977 Ultrasonics Symposium Proceedings, #77CH1264-1SU, p. 124.

APPENDIX B

PROJECTION OF COMPOSITE FOR ACOUSTIC EMISSION SENSORS

W. A. Schulze
Pennsylvania State University

Projection of Composite for Acoustic Emission Sensors

W. A. Schulze

This paper attempts to project the possible application of composite piezoelectric materials developed for low frequency hydrostatic sensing to the detection of moderate frequency acoustic emission. Two studies in addition to the extensive low frequency hydrostatic work* have shown composite material to perform well as a very broadband resonator* and a transducer for medical ultrasound. It is unfortunate that the ultrasound study is of a proprietary nature and may not be disclosed until completion except to state that the results are encouraging.

More detailed explanations of the workings of the various composite materials can be found in the reprint packet included with this paper. In general, the composites consist of a piezoelectrically active PZT phase and a bonding polymer phase. The effect of the polymer phase was for low frequency hydrostatic signals to lower the material permittivity and transfer force to the PZT phase which maintains a large charge response in spite of the reduction of active material. This produces a material with a small d_{31} when compared to d_{33}. The simplest form of this composite (Figure 1) is known as a 3-1 material and consists of PZT columns running along one axis and polymer extending along all three axes. In this case, each PZT column can be pictured as having an area of polymer (more compliant than the PZT) which distorts and transfers stress to the PZT so that the total stress is greater than that which would come from the pressure wave. The result is an increase in piezoelectric g or voltage coefficient. With a sufficient distance between the piezoelectric elements, the composites can be considered as an assemblage of independent elements. This concept was utilized in the broadband resonator, where a 3-1 composite cut in a wedge (Figure 2) becomes an assemblage of independent resonators of different frequencies.

*Sponsored by the Advanced Research Projects Agency (DOD), ARPA, order no. 3203 and Office of Naval Research Contract N00014-76-C-0515.

Composites for AE

There are three forms of the composites studied at Penn State that may be of interest for sensors of acoustic emission. Two are broadband non-resonant devices utilizing PZT or a more sensitive but less developed material (SbSI). The third would be to develop a multi-element resonant device similar to the broadband resonators.

Non-Resonant 3-1 PZT Composites

To cover the 0.1 to 2 MHz band proposed for this study, a non-resonant soft PZT element would have to be less than 1 mm thick. This would yield a sensitivity of less than -110 db re 1V/ubar, when operating in a voltage mode utilizing the piezoelectric g_{33} constant ($\sim$30 x 10^{-3} Vm/N), whereas a resonance device with a more limited frequency range may be between -70 and -60 db. The composites developed for low frequency hydrostatic applications work in a non-resonant mode had a sensitivity of about 35 db above solid PZT. This large increase is possible because PZT is much less sensitive to hydrostatic stress than axial stress (-17 db). With this consideration, a 1 mm thick composite could be expected to have an axial sensitivity on the order of -90 db re 1V/ubar over the desired frequency range.

The composite could be pictured as an assemblage of PZT rods surrounded by polymer (Figure 1). The poling would be along the rod axis (thickness of the transducer). The rods would be 0.5 mm in diameter and occupy only 30% of the surface area. The composite would have a permittivity of 250, piezoelectric d_{33} of 200 x 10^{-12} C/N, density of 3.0 gr/cm^3, a mechanical Q of 8 and an acoustic impedance of about 10 x 10^5 gr/cm^2 sec.

The positive aspects of this composite are: (a) it is naturally damped and would not require an attenuating backing; (b) the average acoustic impedance

approaches that of aluminum and might give good matching; (c) the moderate permittivity does not require a low capacitance preamplifier; (d) the composite could conform to surfaces depending on the type of polymer.

The negative aspects are: (a) a projected low sensitivity to shear waves; (b) a limitation in area to minimize phase differences between elements at higher frequence; (c) possible low sensitivity necessary to achieve bandwidth. It is also not known how well the force transfer mechanism (polymer to PZT) will operate with the composite in contact with a rigid interface instead of the compliant boundary (water) for which the material was developed. It is quite possible, however, that the solid surface will apply all the stress to the rigid PZT and yield a maximum value.

Non-Resonant 3-1 SbSI Composite

In structure, this composite is the same as the PZT device described previously but utilizing a less developed active material (SbSI). The SbSI is in the form of oriented single crystal needles; therefore it exhibits the maximum properties of the material. In the pure form, SbSI has a ferroelectric-paraelectric phase transition at 20°C with a maxima in both permittivity and piezoelectric properties. Embedded in epoxy, the piezoelectric maxima is lowered 15°C below the permittivity peak, giving a broad region of high piezoelectric voltage coefficient ($g_{33} \simeq 100 \times 10^{-3}$ Vm/N) below 15°C. Thus, yielding a material 3-4 times more sensitive than soft PZT with a sufficiently high permittivity (about 650) that does not demand special amplifiers.

The useful working range of SbSI may be modified by adding dopants like S, O, and I, or possibly by altering the fabrication of the crystals and composite. To render this material useful, it would first be necessary to

grow modified crystallites with an increased transition temperature. Once this is accomplished, the anticipated composite should have a broadband response in the range of -80 db re 1V/ubar.

Resonant PZT 3-1 Composite

This device would be very similar to the non-resonant PZT transducer, but the thickness would be varied to produce resonant elements ranging from 0.1 to 2 MHz. Such a device would require a thickness variation of about 1 cm to 1 mm. This use of resonant elements should raise the sensitivity range into that of resonant devices, -70 to -60 db re 1V/ubar.

Such a device has not been built but experience would suggest the following design. The composite should contain many thin rods, perhaps 0.2 mm in diameter, and be contained in a compliant-attenuating polymer. If 20% of the volume were PZT, the spacing would be 0.5 mm between centers, giving 400 rods per square centimeter. The closely spaced thin rods are necessary to minimize the difference in resonance frequency between rods in order to maintain a uniform frequency response. The angle of thickness change would be less for the high frequency region and become steeper in the low frequency region to maintain a constant bandwidth change across the sample (Figure 3). Because of the large variation in thickness, the high frequency regions would have a much higher impedance than the low frequency region. For this reason, it is suggested that a first design be circular with the high frequency region in the center and the thickness increasing toward the perimeter. The area of the low frequency material would increase as a function of the radius and help offset the increase in impedance with thickness. The circular design should be omnidirectional and also have advantages in maintaining small phase differences between elements. The low frequency elements are the most separated, but

operate on the largest wavelength signals. A one-centimeter diameter element would have about 35° maximum phase difference between opposing elements.

Detection of Shear Waves

Preliminary experiments have been conducted in the detection of shear waves and longitudinal waves. The device was again fabricated from PZT rods, but in this case the rods lay along all three orthogonal axes (Figure 4). As in the non-resonant case, the device was sensitive to longitudinal waves through the rods perpendicular to the surface, but also generated a voltage on the rods parallel to the surface. The ratio was about 4:1.

A shear wave directed into the transducer generates a voltage at least twice as large as the rods oriented parallel to the axis of polarization as on the rods perpendicular to the polarization.

Summary

The ferroelectrics group at Penn State has an extensive background in the preparation and characterization of ceramic and single crystal materials and resulting devices. We have pioneered the use of composites for hydrostatic low frequency application and in the process developed the necessary fabrication procedures to be applied to a variety of composites. At the present time we are developing a joint program with faculty of the Polymer Science Department to add the needed expertise to select suitable matrix materials for the various applications.

The several exploratory studies that have been launched into moderate and high frequency applications have offered encouragement that suitably designed composites may have properties unattainable from single phase material. The combination of piezoelectric ceramic and polymer of different sizes, shapes, percentages, and stiffnesses gives a broad variety of composite acoustic and electrical responses.

Composite materials have been produced in both non-resonant and very broadband resonant form with piezoelectric voltage sensitivities greater than that of pure PZT. With proper arrangement of the piezoelectric elements, a device may be made sensitive to longitudinal or shear waves or both, with some determination of the shear wave polarization.

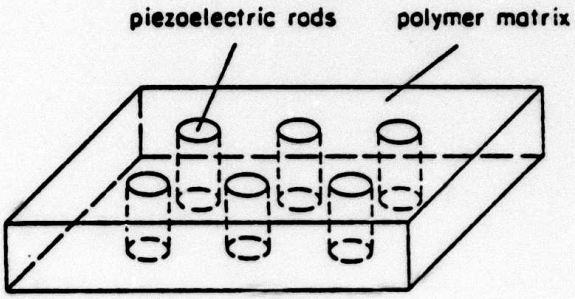

Figure 1

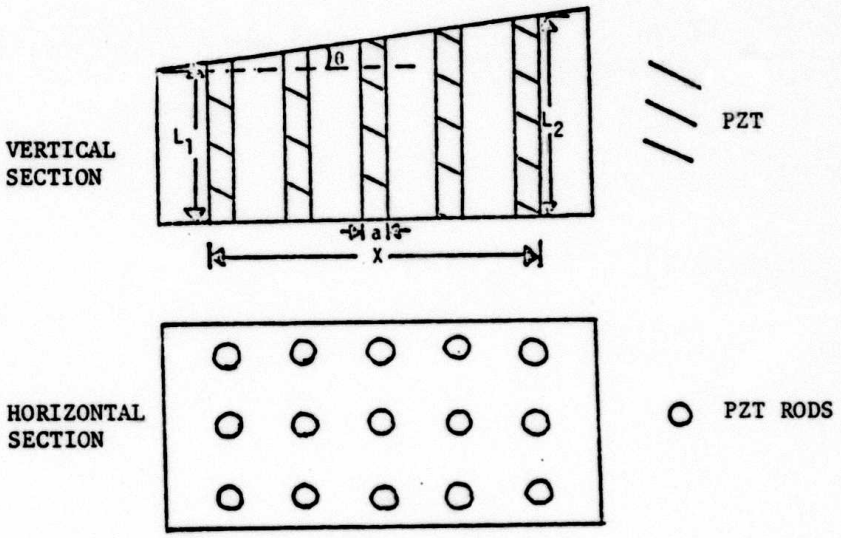

Figure 2

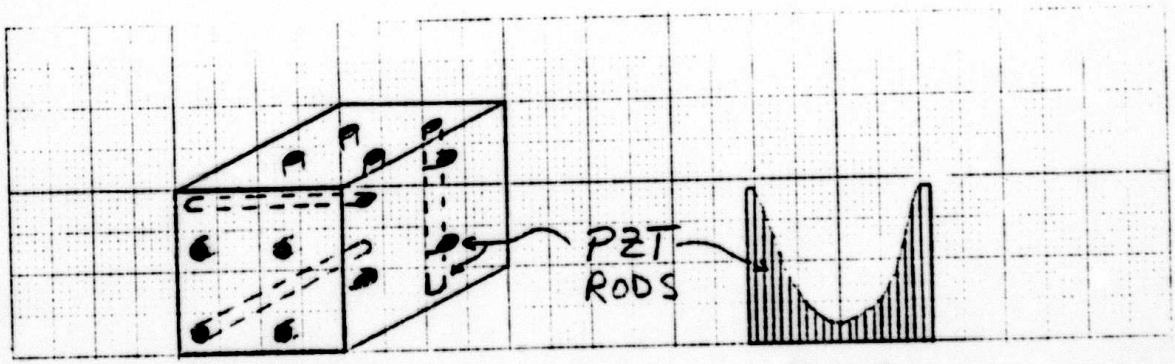

Figure 3

Figure 4

APPENDIX C

ASSESSMENT OF ELECTROMAGNETIC TRANSDUCERS FOR INFLIGHT MONITORING OF ACOUSTIC EMISSION

B. Thompson
Ames Laboratory

ASSESSMENT OF ELECTROMAGNETIC TRANSDUCERS FOR INFLIGHT MONITORING OF ACOUSTIC EMISSION

B. Thompson

1. Present Status of Transducer Concept

a. Physical Principles

The EMAT (Electromagnetic-Acoustic Transducer) is a transducer whose operation is based on physical principles similar to those responsible for the operation of electrical motors and generators. The probe consists of two physical elements: a coil of wire and a magnet. The principles of operation are perhaps most easily understood when the transducer acts as a generator. A dynamic current is applied to the coil and the probe is placed near to the surface of a metal part in which the waves are to be generated. Eddy currents are induced in the metal surface and these experience a Lorentz force due to the presence of the magnetic field. Ultrasonic waves are launched into the material as a reaction to this force.

Considerable effort has been devoted to developing a detailed understanding of the transduction phenomena. A question of considerable interest to the physics community is the mechanism by which the force is transferred from the electrons to the lattice. Both collision and Coulomb interactions appear to play a major role. However, their relative contributions are unimportant for engineering considerations since it is found that the Lorentz force is completely transmitted to the lattice by whichever mechanism is dominant for a particular probe configuration. Thus the wave amplitudes and radiation patterns can be obtained by computing the response of an elastic solid to body forces of the form

$$\vec{f}_L = \vec{J}_\omega \times \vec{B}_0. \qquad (1)$$

where $\vec{J}_\omega$ is the induced eddy current density and $\vec{B}_0$ is the magnetic induction (usually static) induced by the permanent magnet.

The reception process, which is of course of primary interest in acoustic emission applications, requires further discussion. When an ultrasonic wave strikes a metal surface in the presence of the static magnetic field established by the EMAT, electrons which are moving with the lattice cut through lines of flux and thus experience an EMF proportional to $\vec{v} \times \vec{B}_o$, where $\vec{v}$ is the mean velocity of the material. The electron motion is modified in response to this force. The positive ions experience a similar but opposite force, but due to their higher mass and lower mobility, they are relatively undisturbed. As a consequence of the modified motion of the electrons, electromagnetic fields are set up which can be detected as a voltage induced in the EMAT coil.

Again, a detailed discussion of the microscopic details of this process requires a considerable level of effort. Fortunately, the EMAT's are reciprocal devices, and this is not necessary. Circuit models can be devised for the generation case which are equally applicable when the devices are used as receivers. These models will be discussed in greater detail in a following section.

All of the foregoing discussions apply to the case of non-magnetic metals. For iron, steel, or other magnetic materials, magnetostrictive forces are present in addition to the Lorentz forces,[1,2] and a discussion of transduction principles becomes more complex. Since these materials are generally avoided in aircraft components which are monitored by acoustic emission, a discussion of these phenomena will not be given.

b. Transducer Types for Coupling to Different Mode Types

An important advantage of EMAT's is the fact that their structure can be tailored to couple to a wide variety of wave types and polarizations. For any type of transducer, particular waves are selected by arranging the physical structure of the probe so that its induced stress pattern matches, as closely as

possible, that of the wave. For piezoelectric transducers, generation of other than simple wave types can require the fabrication of piezoelectric ceramics of complex shapes and suppression of spurious mechanical resonances of the resulting structure, neither of which is an easy task. On the other hand , the coils of EMAT's can be wound in a variety of complex shapes and such well developed technologies as printed circuit techniques can be used to great advantage where appropriate. The static magnetic field can also be shaped, although the possible patterns that can be realized are not as great in this case since, as for piezoelectric probes, fabrication again requires machining ceramic magnets into particular shapes.

The major fundamental constraints that exist in EMAT design are imposed by Maxwell's equations. Thus, for example, the static bias field must have zero divergence and curl within the metal. For example, if $\hat{z}$ is in the direction of the surface normal, this implies that $\partial Bz/\partial x = -\partial Bx/\partial z$. One might imagine trying to design a magnet with a "pencil beam" of localized, normal magnetic field. However, this would be impossible since, at the edge of the beam $\partial Bz/\partial x$ would be large and hence $\partial Bx/\partial z$ would also be large and Bx could not be zero. Thus careful attention to fringing fields is necessary. The induced eddy currents are constrained to flow in closed paths. This follows since the second term in the equation of current continuity, $\vec{\nabla} \cdot \vec{J} + \partial\rho/\partial t = 0$, is essentially zero in a metal. Hence one should consider the location of the return (or fringing) eddy currents when designing a probe.

Several of the probe types that have evolved are shown in Fig. 1. One of the simplest probes is the spiral coil EMAT shown in part a. Inspection of the directions of currents and fields shows that this coil generates shear waves normal to the metal surface. However, these have a radial polarization which, among other things, implies that there is an on-axis null in the radiation pattern in the far field. Thus null can be removed by adopting the design shown in part b,

and longitudinal waves can be launched normal to the material surface using the one shown in part c.

Beams propagating at angles to surfaces are generated using transducers with periodic structures. Fig. 2a shows the meander coil EMAT in which the magnet is uniformly polarized and the coil is wound back and forth with a periodicity D. When the frequency is selected such that

$$f = V_R/D, \tag{2}$$

this configuration launches Rayleigh waves, since the signals launched from each coil element add coherently. If a higher frequency is selected, then angle beams are launched[3] at the angle with respect to the surface normal

$$\phi = \sin^{-1} V/fD \tag{3}$$

where V is the velocity of the wave of interest (longitudinal or shear).

Figure 2b shows a second periodic probe, the periodic permanent magnet EMAT. Here the coil is uniform and the magnets are periodic, producing a periodic driving force as in the meander coil EMAT. There is, however, one important distinction. The forces of the meander coil are in the plane of Fig. 2a, so that Rayleigh, Lamb, vertically polarized shear waves, or longitudinal waves can be launched. However, the forces of the periodic permanent magnet EMAT are perpendicular to the plane of Fig. 2b so that only horizontally polarized shear waves are launched. This is a wave type which is difficult to couple to with conventional piezo electric probes without establishing a solid bond to the past.

In summary, EMAT's can be constructed which couple to all wave types. These can generally be designed to strongly reject other types as will be discussed below.

c. EMAT Sensitivity

An EMAT can generally be represented by the equivalent circuit shown in Fig. 3. Two closely related descriptors of efficiency are often used; the transfer impedance and the transduction efficiency.[4] The former is defined as the ratio

of open circuit received voltage to driving current for a pair of identical probes. That measure is particularly useful in flaw detection applications. The transduction efficiency, defined as the ratio of power delivered to an electrical load to the incident acoustic power, is more appropriate for an acoustic emission probe. For a spiral coil, this is given in MKS units by[4-5]

$$E = \frac{4\, n^2\, B_o^2\, R_o A}{\rho V |Z+Z_o|^2} \qquad (4)$$

where n is the turn density (turns/meter) of the coil, B_o is the static bias, R_o is the resistive component of the load, A is the coil area, ρ is the metal density, V is the shear velocity in the metal, Z is the coil impedance, and Z_o is the load impedance, including any tuning elements which resonate the inductance of the coil. For the case of the meander coil, the result is

$$E = \frac{4\omega B_o^2 N^2 w R_o}{|Z_o+Z|^2 \rho V^2 p} \qquad (5)$$

where N is the number of periods in the meander coil, w is its width, V is again the shear wave velocity, and p is a numerical factor[1] which varies with Poisson's ratio and has a value of 7 when Poisson's ratio is 0.3. Similar formulae apply to the periodic permanent magnet EMAT shown in Fig. 2b,[2] and the bulk wave EMAT's shown in Figs. 1b and 1c.

Evaluation of Eqs. (4) and (5) for practical parameters, including values of B_o which can be relized with lightweight rare earth permanent magnets, show that efficiencies are typically on the order of -50dB, a value significantly lower than that of piezoelectric probes. This use of the EMAT implies reduced sensitivity. The exact amount of the reduction depends upon the performance of the piezoelectric probe under consideration. Taking 10dB as an estimated loss of a standard commercially available probe (and recognizing that lower values can be realized in custom devices), the EMAT is seen to be 40dB lower in sensitivity.

This number is, of course, a serious limitation for the detection of weak signals, and for those applications in which conventional probes have marginal sensitivity, EMAT's should not be considered. However, in other cases acoustic emission signals are quite strong and the mode selectivity, shear wave sensitivity, high temperature, couplant free characteristics of EMAT's may be of greater significance than their low sensitivity. By way of comparison, it should be noted that the sensitivity of EMAT's is roughly comparable to that of capacity microphones,[7] which are often used in laboratory studies of acoustic emission.

The minimum detectable acoustic power is determined by comparing the electrical signal output of the EMAT to the thermal noise power $4kTR_o\Delta f$. From Eq. (4) one finds that for the spiral coil EMAT the result is

$$P_{a_{min}} = \frac{kT\rho V|Z+Z_o|^2\Delta f}{n^2B_o^2A} \qquad (6)$$

while Eq. (5) shows that the equivalent result for the meander coil EMAT is

$$P_{a_{min}} = \frac{kT\rho V^2p|Z+Z_o|^2\Delta f}{\omega B_o^2N^2W} \qquad (7)$$

As would be expected, these results show that measurement made at high temperature, on high acoustic impedance materials, using high electrical impedance probes, operating at broad bandwidths, have sensitivities that are relatively low (high minimum detectable acoustic power) with respect to those of systems with high magnetic bias fields and coil turn densities.

Two additional comments should be made regarding sensitivity. First, there are in general lift-off effects which degrade EMAT efficiencies in many applications. However, these are relatively unimportant for fixed probe measurements. Second, a number of other second order effects occur which degrade efficiencies below the values quoted above. Typically, these amount to no more than 10dB.

d. EMAT Bandwidth

Since EMAT's contain no mechanically resonant elements, there are no intrinsic factors limiting bandwidth. The major restrictions are associated with the electrical bandwith of coil and receiving electronics and with elastic wave radiation conditions. The electrical bandwidth enters through the factor $|Z+Z_0|$ which appears in the preceding formulae. The coil are usually inductive and sufficiently far below any self resonances, $z \sim R+j\omega L$. There is thus a slow roll off of efficiency versus frequency unless an extremely sophisticated matching circuit is used. Other than this effect, the coils such as those shown in Fig. 1 which detect longitudinal or shear waves propagating perpendicular to surfaces are quite broad band. Operation from 0.1 to 10 MHz can be readily realized.

For the periodic transducers, another effect must be considered. As noted in Eqs. (2) and (3), beams can be directed in selected directions by tuning the frequency so that the signals detected in the elementary portions of the transducer add coherently for waves received from particular directions. This implies a narrowed bandwidth since waves of other frequencies coming from the same direction will not necessarily add in phase.

For the case of Rayleigh waves, the effect is straightforward. The efficiency is proportional to

$$\{\sin[\pi L\Delta f/v_R] \;/\; [\pi L\Delta f/v_R]\}^2$$

which has a full 4dB bandwidth of V_R/L where V_R is the Rayleigh wave velocity and L is the transducer length. Thus a long transducer will have a narrower bandwidth since the wavelength must be more precisely defined in order for the wave to stay in phase under the entire length of the transducer. A broad band probe will have a small value for L, which is equivalent to a small number of fingers N. It will thus have a lower sensitivity. The product of minimum detectable signal amplitude times bandwidth is in fact a constant.

For angle beam probes, the situation is slightly more complex since the angle of maximum sensitivity is a function of frequency. These probes are broad banded in the sense that they can detect energy having many different frequency components. However, each component is optimally detected at a different angle, in accordance with Eq. (2). Thus broad band detection does not imply that all frequency components of waves coming from a particular direction can be detected. If the angle of illumination is fixed, a result similar to that for Rayleigh waves will hold.

e. Beam Patterns

The beam patterns of EMAT's can be readily computed since the coupling is precisely specified by Eq. (1). For a spiral coil EMAT, a radially polarized shear wave is launched or detected normally to the metal surface. The beam will spread in accordance with the usual laws of diffraction, and will have the property that there is a null in the on-axis radiation (or reception pattern). The structures shown in Figs. 1b and 1c couple to waves which have a plane polarized character. They will have radiation patterns quite similar to that of conventional piezoelectric transducers. Details for one particular configuration have been developed by Kawashima.[8] For the case of plane polarized shear probes, polarization purities of greater than 40dB have been reported.[9]

The angle beam radiation patterns of meander coil and periodic magnet EMAT's have been studied in detail by Pardee and Thompson.[10] These results show that there are a variety of side lobes and grating lobes whose existence must be recognized and controlled.

F. Present Status

The present status of the technology discussed above is relatively advanced. Working models of all of the probes discussed above have been demonstrated in the laboratory and, in many cases, incorporated in prototype systems.[11] The probes

have proved to be rugged and durable and can withstand broad ranges of temperature and shock. Their physical size and weight is controlled by that of the magnet. A typical rare earth magnet has dimensions on the order of $(1/2 \text{ in.})^3$ to $(1 \text{ in.})^3$ and will produce a normal field of about 3kG. On line experience has been reported in both England and the Soviet Union.[12] New applications are usually explored via a sequenced program of feasibility demonstration, prototype construction and demonstration, and delivery of fully operational hardware.

g. Summary of Applicability to Acoustic Emission

EMAT's are applicable to the detection of acoustic emissions in cases where their sensitivity is sufficiently high. Wehrmeister has demonstrated this for the case of acoustic emission monitoring of multi-pass submerged-arc welding.[13] Primary advantages include the ability to operate without couplant and at extremes of temperatures. Probes can be designed which couple to a variety of mode types greater than that easily detected by other probes. In aircraft, the design of probes optimized to detect the modes of wing skins or other sheet structures should be considered since this is the primary mode by which energy propagates from the emission source to a remote structure.

References

1. R.B. Thompson, "A Model for the Electromagnetic Generation of Ultrasonic Guided Waves in Ferromagnetic Metal Polycrystals," IEEE Trans. on Sonics and Ultrasonics SU-25, 7 (1978).

2. R.B. Thompson, "Mechanisms of Electromagnetic Generation and Detection of Ultrasonic Lamb Waves in Iron-Nickel Alloy Polycrystals," J. Appl. Phys. 48, 4942 (1977).

3. T.J. Moran and R.M. Panos, "Electromagnetic Generation of Electronically Steered Ultrasonic Bulk Waves," J. Appl. Phys. 47, 2225 (1976).

4. R.B. Thompson, "A Model for the Electromagnetic Generation and Detection of Rayleigh and Lamb Waves," IEEE Trans. on Sonics and Ultrasonics SU-20, 340 (1973).

5. R.B. Thompson, "Electromagnetic, Noncontact Transducers," 1973 IEEE Ultrasonics Symposium Proceedings (IEEE, New York, 1973), p. 385.

6. C.F. Vasile and R.B. Thompson, "Excitation of Horizontally Polarized Shear Elastic Waves by Electromagnetic Transducers with Periodic Permanent Magnets," J. Appl. Phys. 50, 2583 (1979).

7. R.B. Thompson, "Noncontact Transducers,"1977 IEEE Ultrasonics Symposium Proceedings (IEEE, New Yor, 1977).

8. K. Kawashima, "The Theory and Numerical Calculation of the Acoustic Fields Exerted by Eddy-Current Forces," J. Acoust. Soc. Am. 60, 1089 (1976).

9. H. Saltzburger, IZFP, Saarbrücken, West Germany, private communication.

10. W.J. Pardee and R.B. Thompson, "Half-Space Radiation by EMAT's for Non-Destructive Evaluation," J. Nond. Eval. (in press).

11. R. B. Thompson and G.A. Alers, "EMAT Transducers for Ultrasonic Inspection of Structural Materials," Proceedings of the National Electronics Conference--1979 (National Electronics Consortium, Oak Brook, Illinois, 1979), p. 213.

12. H. Frost, "Electromagnetic-Ultrasound Transducers: Principles, Practice, and Applications," in Physical Acoustics, v. 14, W.P. Mason and R.N. Thurston (eds). (Academic Press, New York, 1979), p. 179.

13. A.E. Wehrmeister, "Acoustic Emission Monitoring of Multi-Pass Submerged-Arc Welding," Materials Evaluation 35, 45 (1977).

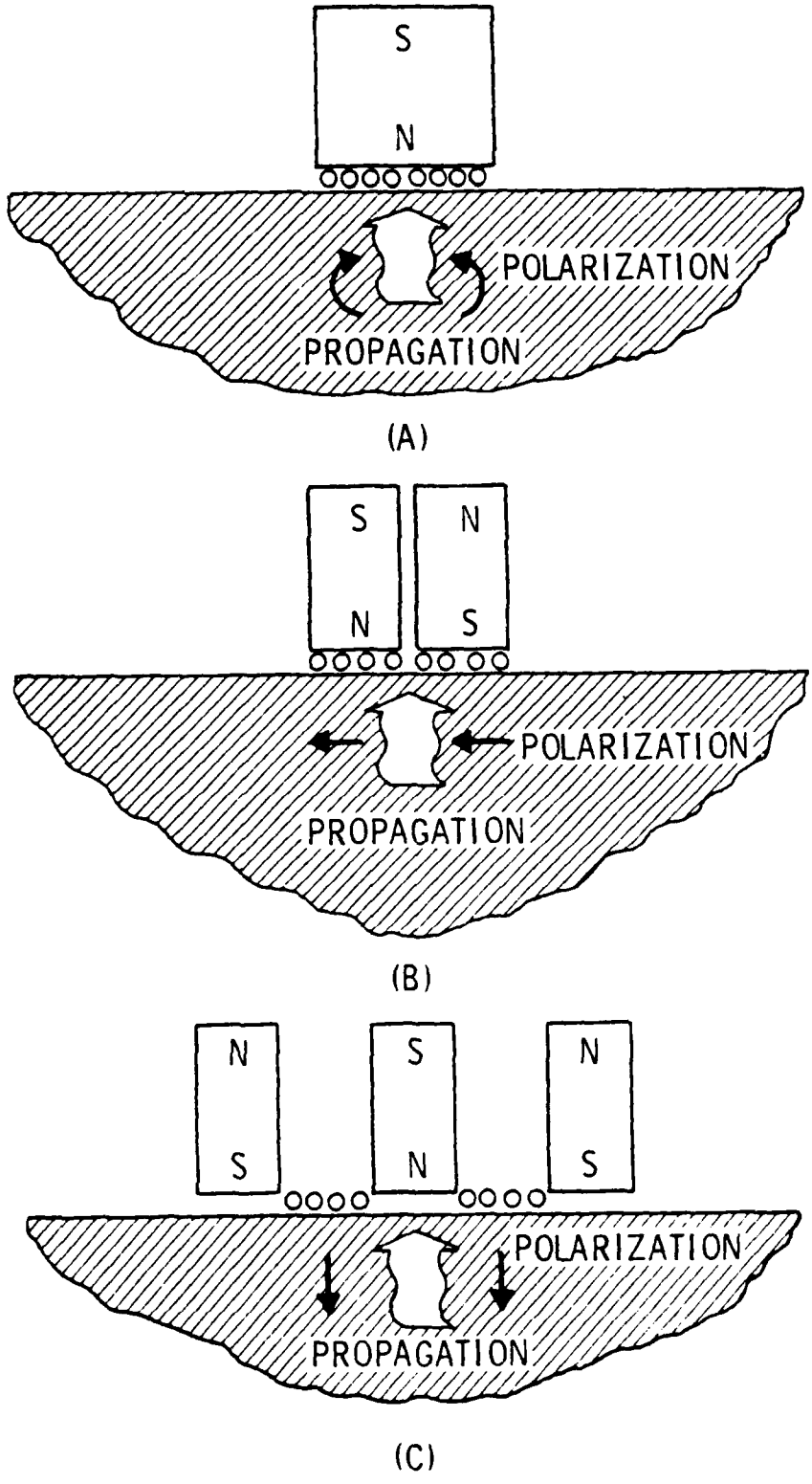

Figure 1 - Bulk Wave EMAT's
a) Spiral Coil for Detecting Radially Polarized Shear Waves
b) Split Magnet for Detecting Plane Polarized Shear Waves
c) Three Magnet Configuration for Detecting Longitudinal Waves

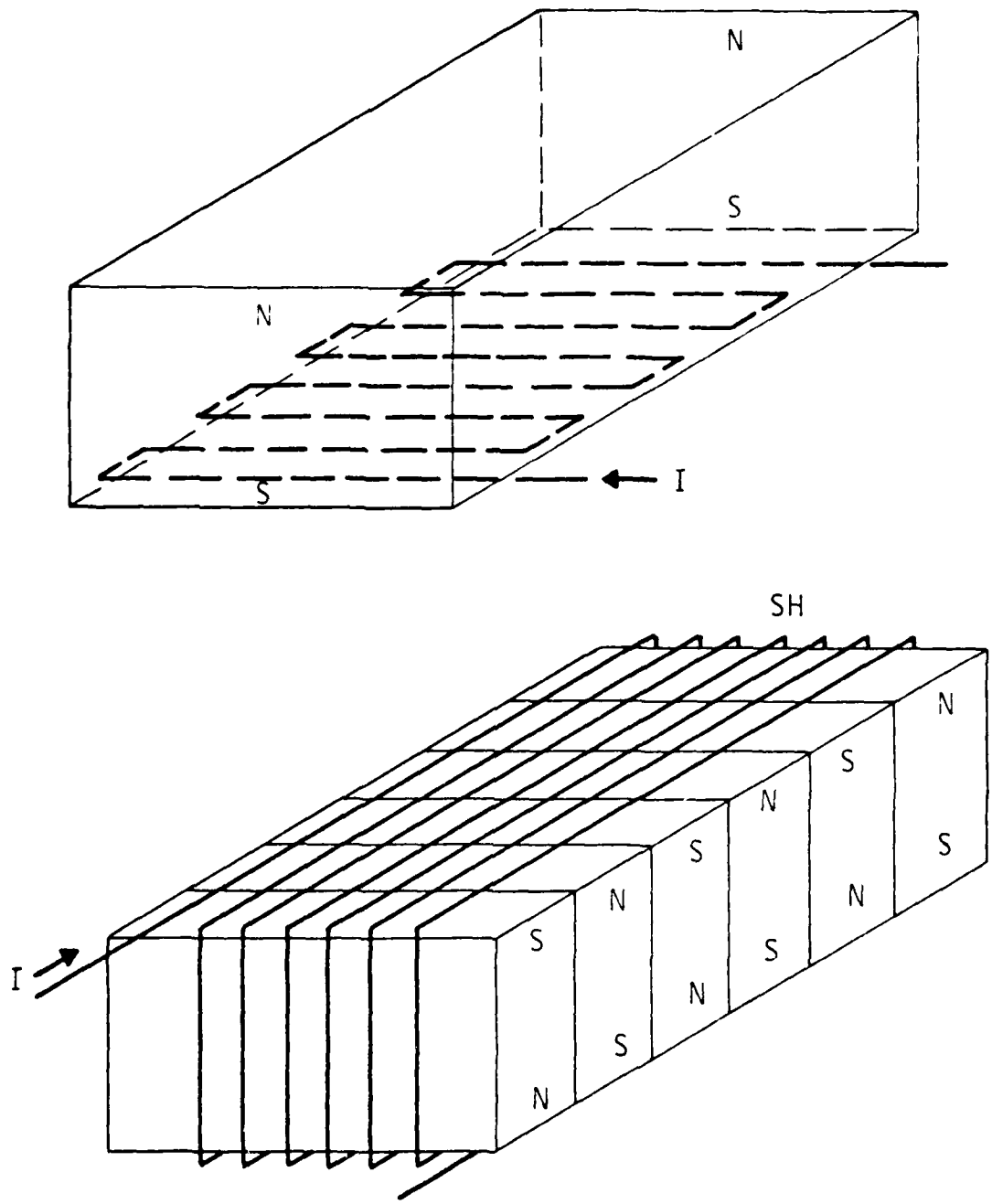

Figure 2 - EMAT Configurations for Coupling to Spatially Periodic Stress Distributions
a) Meander Coil EMAT for Detecting Rayleigh, Lamb and Angle Beams
b) Periodic Permanent Magnet Transducer for Detecting Horizontally Polarized Shear Waves in Plates and Half Spaces

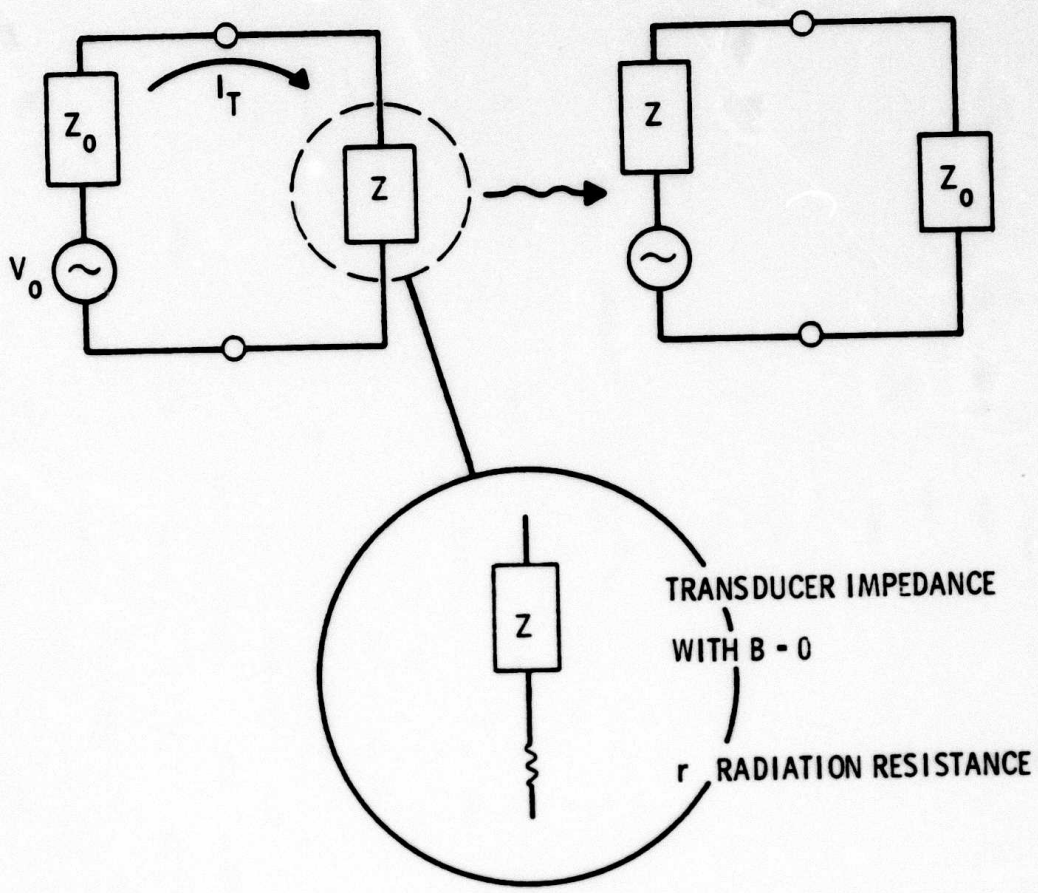

Figure 3 - Equivalent Circuit for EMAT. For all practical purposes, the radiation resistance can be neglected since $r \approx 10^{-6}$ ohms.

APPENDIX D

FET ACOUSTIC TRANSDUCERS

R. M. White
University of California, Berkeley

FET ACOUSTIC TRANSDUCERS

Richard M. White

EECS Dept., U. of California, Berkeley, CA 94720

Report prepared for Battelle Northwest Laboratories

1 August 1980

INTRODUCTION

The term "FET acoustic transducer" is applied to ultrasonic receiving transducers which incorporate a field-effect transducer (FET) with a piezoelectric element, such as a film of zince oxide a few microns thick. These transducers date from the early work of Muller and Conragan (1965). Since the FET and the piezoelectric are formed by integrated circuit techniques, low cost and easy attainment of desired transducer dimensions, and hence response, are among the outstanding characteristics of this device. Since the transducer is made on silicon, it lends itself naturally to being combined with integrated circuit signal-processing devices made in the same silicon substrate. And, finally, the transducer response should be similar from unit to unit because it is possible to dimension the devices quite precisely.

In the report which follows, we summarize the features, state of development, and expected future capability of the FET transducer. We use the format suggested by Battelle, except for the addition of Section 1-E on special characteristics of this transducer.

SECTION 1: PRESENT STATUS OF TRANSDUCER CONCEPT

1-A: Physical principles employed

Two versions of the transducer have been considered, as shown in Fig. 1-1. The upper sketch shows a more or less conventional field-effect transistor (FET) in which a film of piezoelectric zinc oxide has been sputtered over the FET gate at an appropriate time in the manufacturing process. Since the flow of the current I_{SD} between source and drain electrodes is affected by the electric fields in the gate region (which includes the channel through which the source-drain current flows), this device is sensitive to strain of the piezoelectric film. That is, if a constant gate bias potential V_G is applied at the metallic gate, the source-drain current Isd which flows will depend upon both the applied voltage V_G and upon the strain-induced electric fields in the zinc oxide. One may regard the effect variously as resulting from the electric fields of both the metallic gate electrode and the piezoelectric, or one may say that it is the potential at the channel which is important, and that potential depends upon both V_G and the potential difference obtained by integrating the electric field in the ZnO through its thickness. Either accumulation or depletion mode FETs may be used; we have used depletion mode devices primarily.

Fig. 1-2 shows the magnitude of I_{SD} vs. V_{DS} for a particular device of this type. The parameter on the curves is V_G, and for each such value there is a curve for the unstrained (unmarked) and the strained case. The transducer

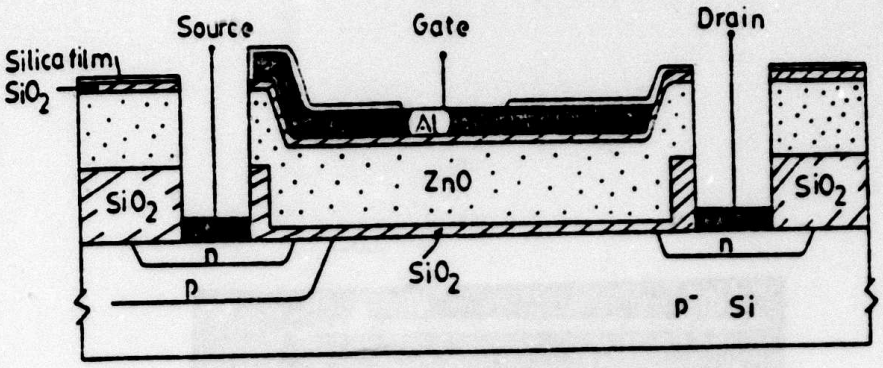

Fig.1-1a. Cross-section of the channel region of the n-channel PI-DMOS transistor.

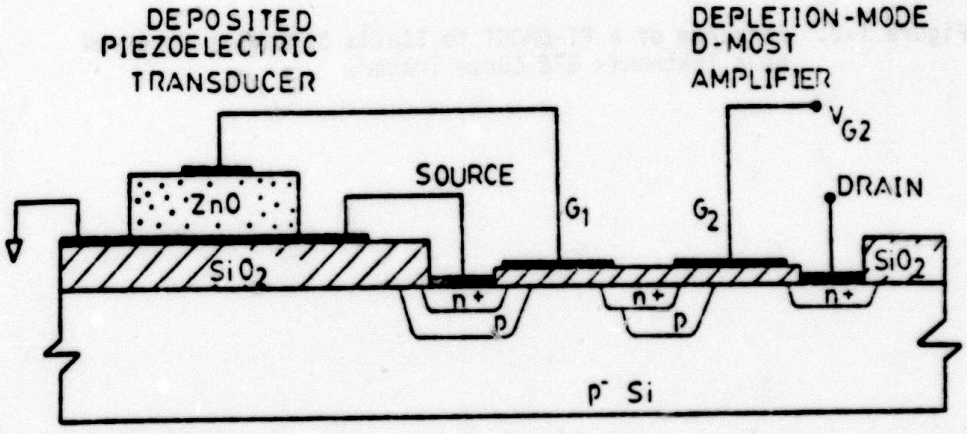

Fig.1-1b. Cross-section of the ZnO thin-film capacitor-coupled dual-gate D-MOS transistor.

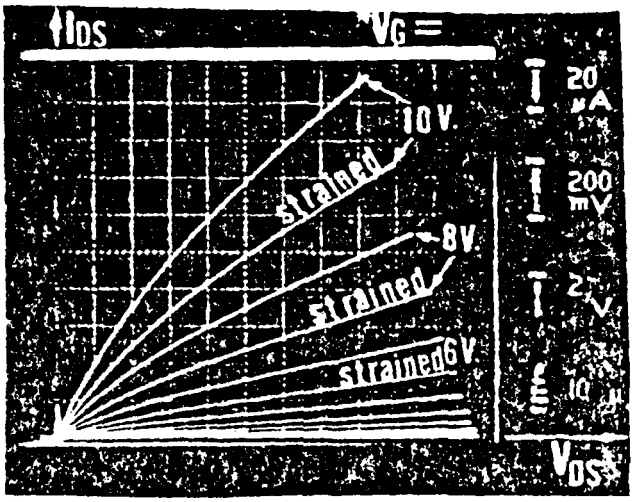

Figure 1-2. Response of a PI-DMOST to Statis Strain as Observed on a Tektronix 576 Curve Tracer.

output is the changing current I_{SD} or the voltage that changing current produces in a load resistor connected to the FET. If one defines a sensitivity for such a device at low frequency as $(\Delta I_{SD}/I_{SD})/S$, where S is the strain at the ZnO film, one finds this "gauge factor" is typically around 100,000, a very large value when compared with gauge factors for conventional strain gauges.

The second arrangement used and shown in the bottom of Fig. 1-1 has the piezoelectric placed adjacent to but not over the FET gate region. Note that in this illustration the FET has two gate electrodes rather than one, for reasons described in Section 1-E below; for the moment, the reader can assume that an ordinary single-gate FET is used here with a ZnO stripe transducer connected to it. There are several advantages to this construction: (1) The FET can be designed optimally to perform its function, and the dimensions of the piezoelectric film can be entirely different from the gate dimensions to permit a desired acoustic response to be achieved; (2) More than one transducing film can be attached to a single FET gate; (3) Conventional commercial FETs can be used and the piezoelectric film can be added as an overlay later; (4) Hybrid structures can be made with the film on one substrate and a small FET silicon die, a few millimeters on a side, attached adhesively to it, and (5) Formation of the piezoelectric film will not degrade the FET performance, since no sputtering has to be

done over the sensitive channel region (this damage sometimes occurred with the ordinary RF sputtering technique used previously; it should be less a problem with the planar magnetron sputtering technique used now).

Fig. 1-3a shows a transducer made as in the upper part of Fig. 1-1; this is the so-called PI-DMOST structure, for "piezoelectric double-diffused MOS transistor". The double diffusion refers to the formation of a very short, and therefore rapidly responding, channel near the source (Fig. 1-1a) formed by a p-type diffusion followed by a heavy n-type (n+) diffusion. The channel itself is only one micron wide while the gate electrode is about 7 microns wide. Fig. 1-3b shows the second type of structure where ZnO was sputtered on an entire commercial wafer of FET transistors and then shaped by photoetching to the desired dimensions. (These photos are all from work done at the University of California, Berkeley.)

A number of equations relating to these devices appear in Table I.

1-B: Sensitivity to bulk and surface waves

The sputtered zinc oxide films are primarily responsive to compression or tension in a direction normal to their plane, since the films have a strongly preferential growth orientation -- the hexagonal c-axis is normal to the sub-

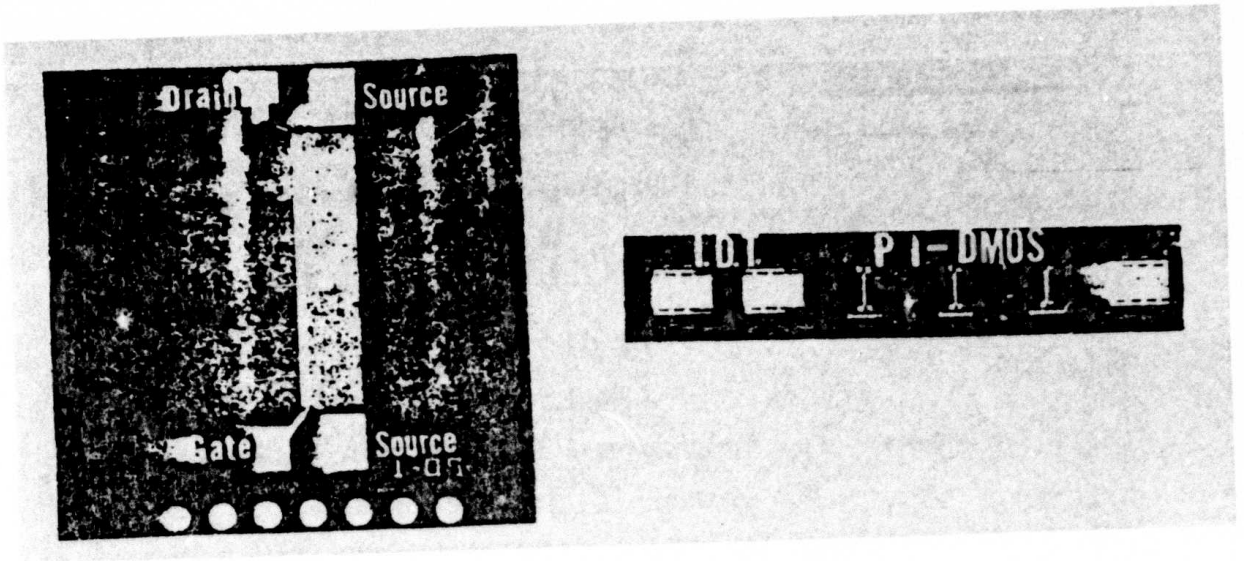

Figure 1-3a. Left: Magnified Top View of PI-DMOS Transducer.
Right: Top View of Integrated Arrangement of PI-DMOS Transducer and Interdigital Transducer as Used in SAW Experiments.

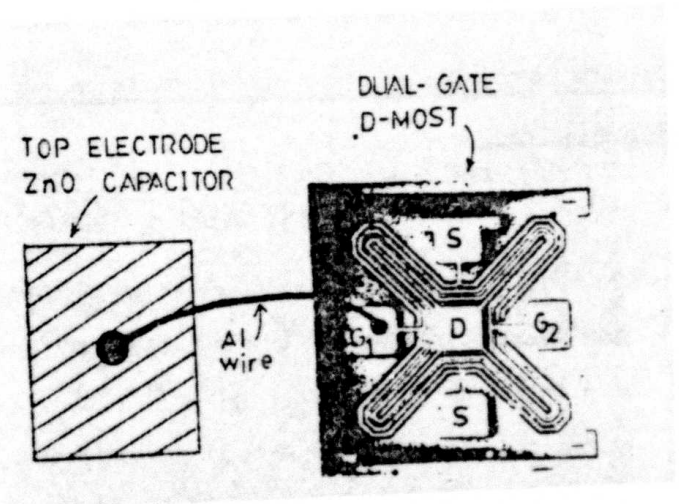

Figure 1-3b. Top View of ZnO Thin-Film Capacitor Connected with Wire to Dual-Gate D-MOST (die cut from wafer of commercial devices).

TABLE I. SOME EQUATIONS RELATING TO ZnO-FET OPERATION

1. FET operation:

Low drain bias: $$I_D = \mu_n \frac{W}{L} C'_{ox}(V_G - V_T)V_D$$

(I_D linear in V_D, conductance proportional to $V_G - V_T$)

Higher drain bias: $$I_D = \mu_n \frac{W}{L} C'_{ox}\left(V_G - V_T - \frac{V_D}{2}\right)$$

Saturation drain bias and above: $$V_{G\,sat} = V_G - V_T,$$
$$I_{D\,sat} = \frac{1}{2}\mu_n \frac{W}{L} C'_{ox}(V_G - V_T)^2,$$

where I_D = drain current, V_G = gate bias, V_D = drain voltage, μ_n = mobility, C'_{ox} = oxide capacitance per unit area of gate, W = channel width, L = channel length, and V_T = threshold voltage.

2. Sensitivity factor for unbacked piezoelectric on support, both being acoustically thin:

$$V_{oc}/T_{3,inc} = -\frac{e_{33}}{\epsilon_{33}} \frac{1}{c_{p,33}K_p} \frac{1-\cos K_p t}{\sin K_p D} \frac{2}{1-j\frac{Z_D}{Z_p}\cot(K_p D)},$$

where V_{oc} = open-circuit voltage, $T_{3,inc}$ = incident normal stress for bulk longitudinal wave, t = thickness of piezoelectric layer, d = thickness of support, $D = t + d$, $K_p = \omega/v_p = 2\pi/\lambda_p$ = propagation constant for wave in piezoelectric, ϵ_{33} = dielectric permittivity of piezoelectric, e_{33} = piezoelectric coefficient of piezoelectric, $c_{p,33}$ = elastic stiffness for piezoelectric. Z_D = acoustic impedance of support, and Z_p = acoustic impedance of piezoelectric.

strate on which the film is deposited. X-ray rocking angle measurements of ZnO films on silicon show a spread of c-axis orientations from the normal of only about ± 0.9 degrees, indicating a highly oriented film.

The films themselves can respond to the types of excitation shown in Fig. 1-4. If the transducer is attached to a flexible cantilever, moving the free end downward as shown (Fig. 1-4a) stretches the film, causing its thickness to reduce and so a piezoelectric output voltage is produced. This flexural arrangement has been used to calibrate the transducer and to test for its low frequency response, as mentioned below in Sec. 1-C. The thickness mode (Fig. 1-4b) has been described above; note that it is simplest to operate the film without backing, so that there is no normal stress on its upper surface. Anaysis of the response in this mode, which would be excited if longitudinal bulk waves were incident on the transducer from below, is cited in Sec. 1-C below. End excitation (Fig. 1-4d) by a bulk longitudinal wave from below would cause a Poisson-coupled change in the thickness of the ZnO film. A nonvanishing output voltage would be obtained in this case only if the film width were substantially less than one wavelength at the frequency of operation.

Surface-wave operation (Fig. 1-4d) deserve special mention because it illustrates how one can obtain directional receiver characteristics. Here an array of integrated

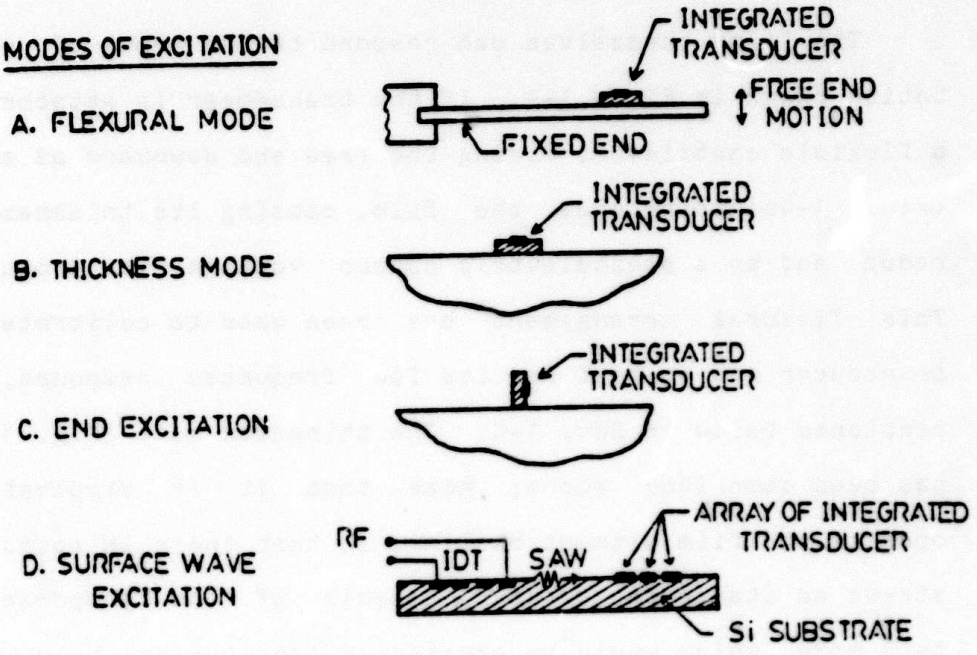

Fig. 1-4. Modes of excitation

transducers is indicated; the individual ZnO stripes are dimensioned and spaced so that their outputs add constructvely at the desired operating frequency. The design consderations are similar to those for the interdigital transducer (IDT) shown here generating the surface acoustic wave (SAW) for measurement purposes, except that here the center-to-center distance for the stripes should be one wavelength.

Sensitivity of these transducers to shear has not been tested yet, to our knowledge. If the shear wave were incident at an acute angle to the transducer surface, there would be a normal component of particle motion and one might expect to observe an output from the ZnO film because of that. Incidentally, this situation is not different from that for any piezoelectric transducer, except that in this case the transducer is thin in terms of wavelengths and so it is usually operating below its fundamental thickness resonance frequency, a fact which simplifies analysis of the response.

Experimentally response has been observed in all these mode (except for that of shear wave incidence) and is describe in Yeh and Muller (1976) and in Kwan (1978). Frequencies ranged from far below one Hertz, in flexural operation, to about 90 MHz in SAW operation.

1-C: Bandwidth and sensitivity of present models

In exploring this transducer we have made devices on standard 0.010-0.015 inch thick silicon wafers, and have also tested ZnO films deposited on glass and on stainless steel sheets having thicknesses as small as 0.002 inches. We have measured response in the flexural mode, where the strain can be calculated from the dimensions and displacement of the free end of the cantilever. We have compared ZnO transducer output under 10 MHz excitation, supplied by a Panametrics PZT transducer, with that of a commercial acoustic emission transducer. We have made a self-reciprocity calibration of our 10 MHz source transducer and used that as a standard. We have looked at the response to the surface disturbance created by the breaking of a pencil lead. And, finally, we have carried out an approximate analysis of sensitivity based on physical principles so as to emphasize the phenomena involved in the devices.

Table II and Fig. 1-5 summarize most of the analysis. We examined the sensitivity factor $V_{oc}/T_{3,inc}$ for different combinations of ZnO thickness, thickness and material of support on which the ZnO is deposited, and substrate material to which the transducer is attached. Aluminum and stainless steel were the materials to which the transducer was assumed to be attached. One notes from either the extreme values of this sensitivity parameter in the Table or from the plots in the Figure that the sensitivity rises rapidly as the ZnO layer thickness increases. Also, silicon

TABLE II. Calculated values of the sensitivity factor $V_{oc}/T_{3,inc}$ at extremes of frequency range 0.2 to 2.0 MHz for various ZnO thicknesses, transducer support materials, and substrate materials.

Piezoelectric	Support	Substrate	ZnO 10 microns thick		ZnO 100 microns thick	
			50 μm support	500 μm support	500 μm support	2500 μm support
ZnO	Stainless steel	Stainless steel	1.13×10^{-9}-1.13×10^{-8}	1.13×10^{-9}-1.13×10^{-8}	1.13×10^{-7}-1.13×10^{-6}	
ZnO	Stainless steel	Aluminum	2.85×10^{-9}-2.73×10^{-8}	2.76×10^{-9}-1.21×10^{-8}	2.73×10^{-7}-1.17×10^{-6}	1.76×10^{-7}-1.89×10^{-6}
ZnO	Silicon	Aluminum	2.85×10^{-9}-2.84×10^{-8}	2.85×10^{-9}-2.63×10^{-8}	2.85×10^{-7}-2.42×10^{-6}	2.78×10^{-7}-2.44×10^{-6}
ZnO	Glass	Aluminum	2.85×10^{-9}-2.87×10^{-8}	2.86×10^{-9}-3.58×10^{-8}	2.87×10^{-7}-3.34×10^{-6}	3.08×10^{-7}-2.54×10^{-6}

Values in boxes in Table represent $V_{oc}/T_{3,inc}$ at 0.2 - 2.0 MHz

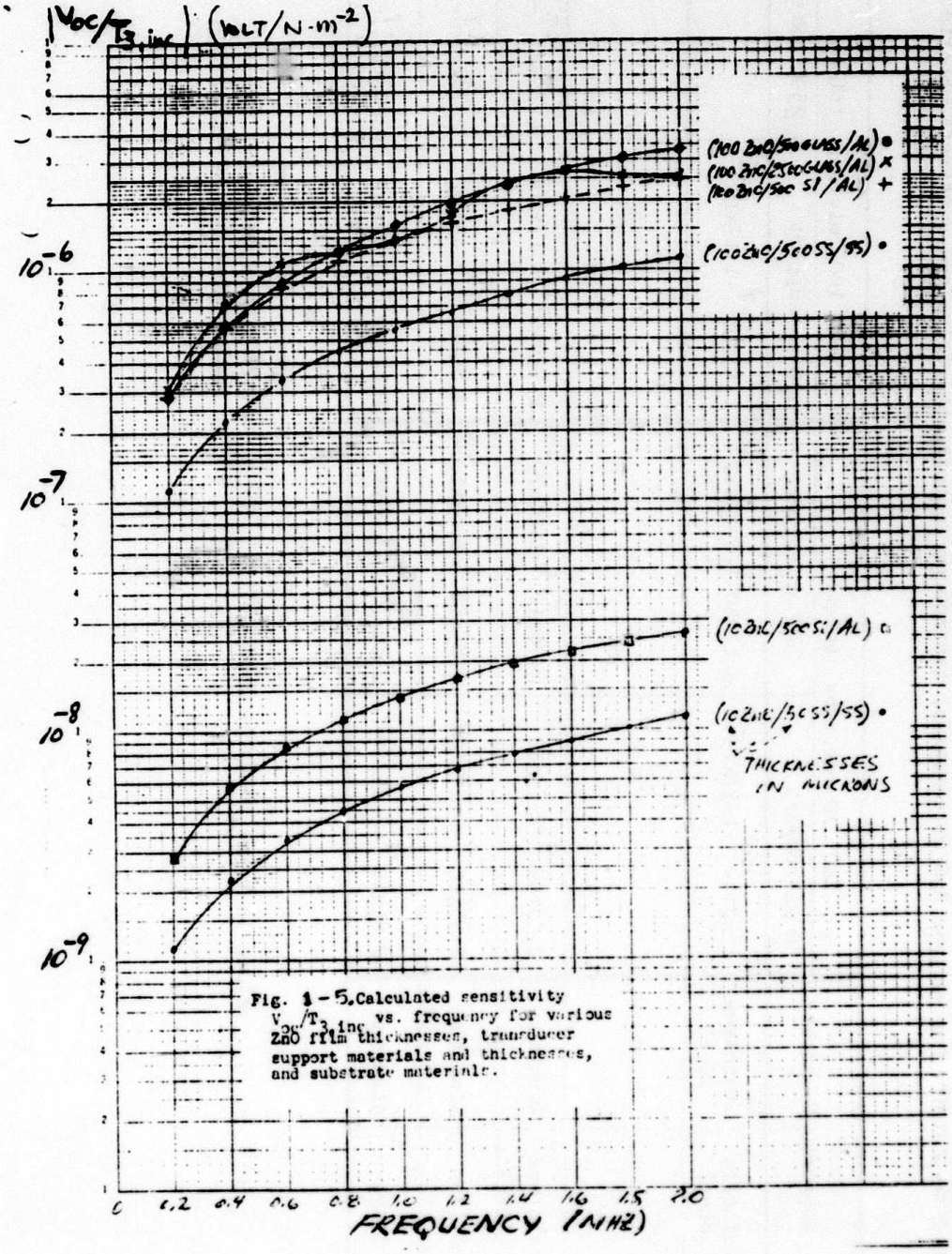

Fig. 1-5. Calculated sensitivity $V_{oc}/T_{3,inc}$ vs. frequency for various ZnO film thicknesses, transducer support materials and thicknesses, and substrate materials.

or glass supports work well in a transducer to be used on aluminum. Incidentally, the open-circuit voltage is the relevant parameter to employ here because the ZnO films are assumed to operate into the virtually infinite impedance of an FET gate. It should also be noted that the receive parameter defined by Callarme at al. (1979) for ultrasonic receiving transducers (Table III) is quite good for ZnO relative to more traditional materials such as lithium niobate and PZT.

In the case of the 2500 micron thick glass supported transducer, the thickness resonance has been shifted down into the operating frequency range; this causes a peak in response to occur within, rather than at the high end of, the range, but the overall magnitude of the response is only slightly increased because the resonance peak is relatively small for this combination of substances. Incidentally, the rising characteristic of the sensitivity will tend to offset the fall with increasing frequency due to ultrasonic attenuation in the substrate materials.

One can show that the sensitivity factor plotted in Fig. 1-5 is proportional, for acoustically thin piezoelectric and substrate thicknesses, to $t^2/(t+d)$, where t is thickness of the ZnO and d is thickness of the support on which the ZnO is deposited. Thus if $t<<d$, the sensitivity factor increases as the square of the piezoelectric layer thickness, making it worthwhile to deposit thick ZnO layers.

Piezoelectric Material	K_t	$\frac{\epsilon^S_{33}}{\epsilon_0}$	C^D_{33} 10^{10} nt/m^2	Transmit Parameter Å/Volt	Receive Parameter per Unit Thickness
PVF_2	0.12	~12	0.82	0.138	12.9×10^{-2}
ZnO	0.29	10.2	22.74	0.066	6.7×10^{-2}
CdS	0.15	9.5	9.59	0.045	5.3×10^{-2}
Quartz	0.093	4.5	8.76	0.02	5.0×10^{-2}
$LiNbO_3$	0.17	29.0	25.2	0.056	2.1×10^{-2}
PZT-4	0.51	635	15.9	1.3	1.7×10^{-2}
PZT-5A	0.49	830	14.7	1.4	1.5×10^{-2}

TABLE III. Characteristics of commonly used piezoelectrics. Transmit and receive parameters apply to longitudinal wave propagation only. Propagation is perpendicular to the plane of PVF_2, along the z-axis for ZnO, CdS, and $LiNbO_3$, along x-axis for quartz, and along the direction of polarization for PZT.

We know of the successful sputtering of ZnO layers 20 microns thick, and there is in principle no reason why thicker layers cannot be obtained, and with them, higher transducer output. Sputtering rates to about 10 microns/hour have been reported (Shiosaki et al. 1978). The limiting thickness may be set by buildup of contamination and consequent loss of orientation during a long sputtering run, or cracking of the film during cool-down owing to the different coefficients of thermal expansion of the ZnO and the support. Certainly a factor of at least three increase over the 10 microns we presently employ should be possible, leading to about an order of magnitude increase in sensitivity.

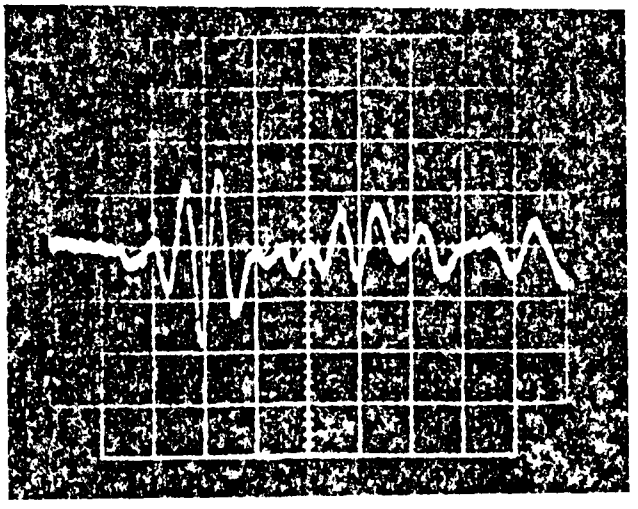

Figure 1-7. Detection of a simulated (pencil-breaker) AE signal by the ZnO transducer. Vertical scale: arbitrary; horizontal: 2 microseconds/division.

Input Equivalent Noise Voltage

For a FET the noise varies with frequency in two characteristic ways. At very low frequencies there is a 1/f flicker noise region, and that blends into the region, dominated by thermal noise of the channel, in which the equivalent input noise voltage per square root of bandwidth is independent of frequency. The bottom of the frequency range of interest here seems generally to be above the 1/f region, and noise voltage characteristics of the order of a few nanovolts/$(Hz)^{1/2}$ should apply through the 0.2 to 2.0 MHz range. It has been established that the ZnO itself introduces noise which is generally below that produced by the FET channel, and so the noise characteristics of the FETs should be dominant.

Response to Simulated Acoustic Emission Source

We have tested the response of a thin-film ZnO transducer to the surface signal from a pencil-breaker source. The output waveform is shown in Fig. 1-7. The transducer consisted of 10 microns of ZnO on a 50-micron stainless steel sheet. The output signal reached nearly 0.9mV. If one assumes a bandwidth of 1.8 MHz and 2 $nV/(Hz)^{1/2}$ equivalent input noise voltage, this yields a signal-to-noise ratio of 340, or about 50 db. The gain of the FET and circuit typically used in these experiments is about 10, and it is essentially constant through the frequency range of interest.

1-D: Beam characteristics and directionality

First we discuss characteristics of the acoustically thin ZnO transducing film, and then consider useful modifications resulting from connecting the film to active semiconductor devices.

In its simplest form of a piezoelectric film and a substrate or wear plate which are both thin compared with an acoustic wavelength, the directionality of the transducer

can be rather simply predicted, and control of it achieved by properly dimensioning the photomask features used to define the active areas of the film. The active areas are the regions beneath a top electrode, typically a thin film of aluminum evaporated in vacuum through apertures in a metal mask, or evaporated and then shaped by conventional photolithography and etching.

The familiar principles determining directionality generally apply to these transducers. For reception of bulk longitudinal waves (as in Fig. 1-1b), as the angle of incidence varies from normal incidence, for a circular transducer whose diameter is much smaller than a wavelength, one would expect a response which was essentially nondirectional but modified by a factor resulting from the gradual decrease of magnitude of the normal component of motion at the free surface as the angle of incidence increases. As the diameter of the transducer increases, directionality involves the product of terms representing the decreasing normal component and the directivity of the circular transducer itself. This behavior has been observed, as shown in Fig. 1-8 in a test where a thin ZnO transducer positioned on the surface of a water bath was irradiated with 167 kHz waves from below.

Connection of two circular ZnO film transducers together to form an array produces the results shown in Fig. 1-9. In this case, a null in the response occurs at roughly

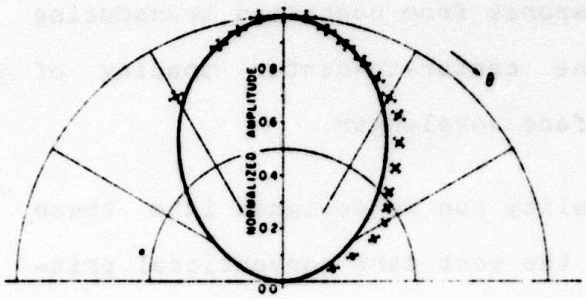

Fig. 1-8. Measured directivity pattern for 0.42cm diameter (equivalent to half wavelength at 167 KHz in water) circular zinc oxide transducing 10 micron-thick film on 0.002 inch thick stainless steel, measured in water bath with 167 kHz signals. Solid curve is plot of equation $\cos\theta\cos^2\frac{\theta}{2}\left|J_1\left(\frac{Ka\sin\theta}{Ka\sin\theta}\right)\right|$ where a=radius of thecircular aperture; K=wave number in water. Data points indicated by points with error bar.

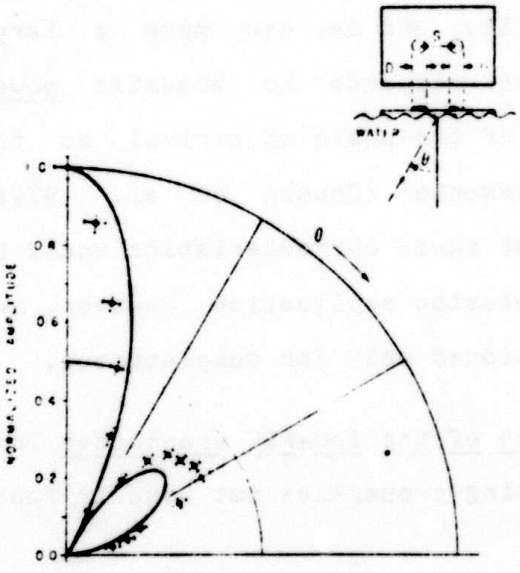

Fig. 1-9. Directivity pattern for two transducers having dimensions given in Fig. 9 with center-to-center spacing equal to 0.84cm, equivalent to one wavelength for 167 kHz waves in water. Outputs were weighted equally and summed. Solid curve represents the function $\cos\left(\frac{\pi s}{\lambda}\sin\theta+\frac{\alpha}{2}\right)\cos\theta\cos^2\frac{\theta}{2}\left|\frac{J_1(Ka\sin\theta)}{Ka\sin\theta}\right|$ where s=center-to-center spacing between elements; α=phase shift between array elements (=0° in this case); λ=wavelength in water. Data points indicated by points with error bar.

30^{o} from the normal, where the outputs of the two transducing regions were of equal magnitude and opposite phase. Similarly, surface wave response from connected transducing stripes is observed when the center-to-center spacing of adjacent stripes is one surface wavelength.

Summarizing, directionality can be designed into these transducers by applying for the most part conventional principles of array design. Realization of designs is simple because the dimensions are established by precisely reproducible photolithographic processes.

The properties discussed thus far in this section are obtained simply by proper shaping of electrodes on the ZnO film and connecting them to a single amplifier for impedance transformation to an output line. If active elements such as the dual-gate FET are used to connect outputs of individual transducing regions to an output circuit, then one can obtain alterable directionality, and one can make a large aperture transducer which responds to acoustic power incident upon it regardless of the phase of arrival at the individual transducing elements (Chuang et al. 1979a, 1979b). It is not clear that these characteristics would be of use in the acoustic emission application, however, and these possibilities are mentioned only for completeness.

1-E: Special characteristics of the ZnO-FET transducer This transducer has some interesting properties not usually found

in conventional transducers. These features, discussed below, result from use of a dual-gate FET, and the fact that the heart of the transducer is a deposited thin film.

(1) Amplitude control

If a dual-gate transistor is used, as indicated in Fig. 1-1b, amplitude control and mixing can be accomplished conveniently in the transducer itself. The second gate, on the right in Fig. 1-1b, can control the current I_{SD} just as the first gate does. Hence in an n-channel depletion mode device which requires no steady gate bias for operation, one can reduce I virtually to zero with a 1-volt negative bias on the control gate. Note that the control voltage does not appear on the signal gate and so there is a desirable separation of these two channels. This amplitude control is shown in Fig. 1-10 where the upper trace is the response of a fully turned-on dual-gate FET to a rather complex bulk longitudinal wave having components around 5 MHz, and the bottom trace shows the gating out of a portion near the center of the trace.

This gating feature could be used for sampling to multiplex a number of transdcers connected to a single output cable. Since the DMOST transistors are capable of high frequency response, one might sample transducers in rotation, in response to a system clock, with sampling pulses short enough to permit reconstruction of the signal waveform com-

AMPLITUDE CONTROL. Top trace shows output of dual-gate sensor in response to acoustic bulk longitudinal wave excitation at approximately 5 MHz with constant DC bias on second gate and signal applied to first gate. Lower trace shows effect of reduced gain near center of trace resulting from an 8 microsecond negative pulse superimposed on the DC second-gate bias. Such amplitude control could be used to deaden receiving transducer during "main bang" of nearby transmitting transducer or to select a portion of the output for display.

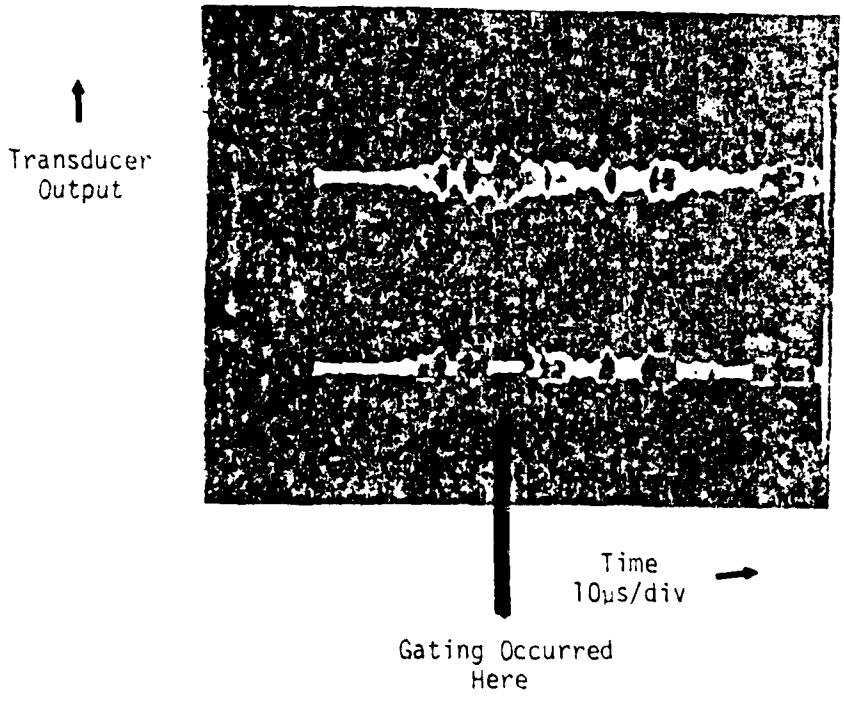

Figure 1-10. Amplitude Control with Dual-Gate Device.

ponents which will lie in the 0.2-2.0 MHz range.

The control gate could also be used for analog amplitude control, for example, to balance transducers at different locations in a structure. And the amplitude control could be used in conventional transmit-receive ultrasonic work to turn off the receiving transducer during input of the "main bang" electrical signal.

(2) Freqency translation (mixing)

Analysis of the dependence of source-drain current I_{SD} for the dual-gate FET is complex (Kwan et al. 1979) but the results show that I_{SD} is proportional to the product of the two gate voltages, at least for small values of those voltages. Thus mixing occurs in the device.

Two examples has been studied, as shown in Figs. 1-11 and 1-12. In the first experiment, the very low frequency response of a dual-gate FET transducer was tested in the flexural mode shown in Fig. 1-1a. By applying a constant-amplitude 50 kHz signal to the control gate (Gate 2), the output was modulated at that frequency, permitting detection of the output to be done conveniently with ac-coupled rather than dc-coupled circuitry. The second exam. shows mixing with a local oscillator at various frequencies so as to produce a 30 MHz "intermediate frequency" output. Efficiency of the dual-gate FET as a mixer is as good as or better than that of good commercial discrete mixer crystals at these

FIG. 1-11. MIXING IN DUAL-GATE DMOS DEVICE.

FREQUENCY TRANSLATION (MIXING).

(A) FREQUENCY SHIFTING WITH PI-DMOST. HERE 50 KHZ CW VOLTAGE WAS SUPERIMPOSED ON THE GATE ELECTRODE OF THE FIRST TRANSDUCER STRUCTURE DURING LOW-FREQUENCY STRAIN MEASUREMENTS. TRANSDUCER OUTPUT IS AT 50 KHZ PERMITTING USE OF LOCK-IN DETECTION AND PLOTTING ON A CHART RECORDER. UPPER TRACE IN PHOTO SHOWS OUTPUT OF TRANSDUCER IN NON-STRAINED STATE; LOWER TRACE SHOWS OUTPUT WHEN STRAIN IS APPLIED (ROUGHLY 8×10^{-5} STRAIN MAGNITUDE). PORTION OF CHART RECORDING BELOW SHOWS CORRESPONDING OUTPUT OF LOCK-IN AMPLIFIER (SHIFT IN BASELINE IS BELIEVED DUE TO DRIFT OF IONS IN GATE OXIDE UNDER INFLUENCE OF DC GATE BIAS).

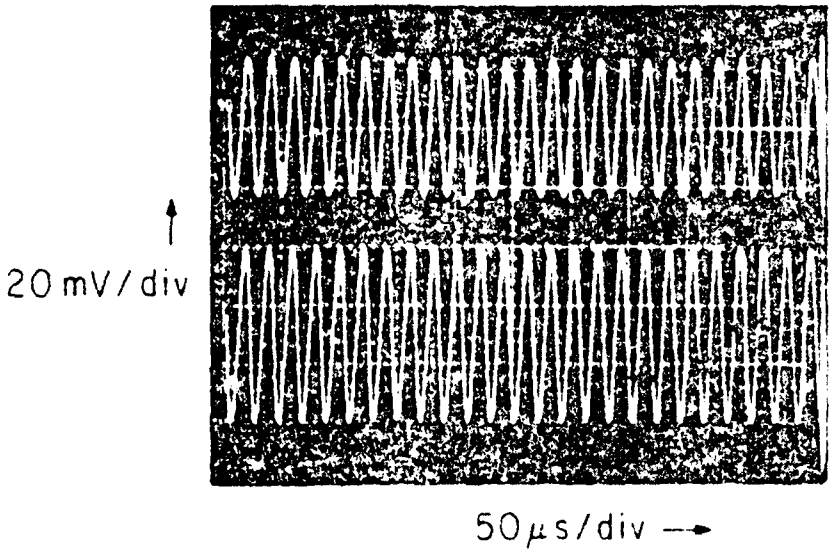

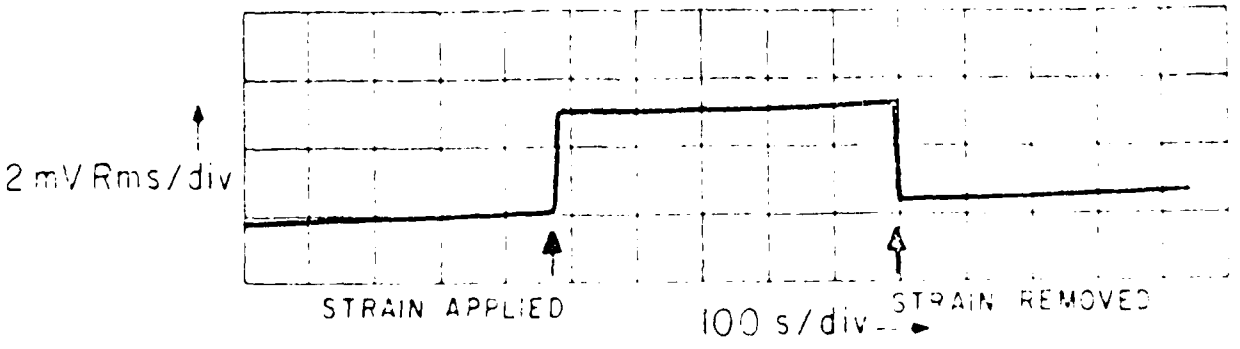

FIG. 1-12. MIXING IN DUAL-GATE DMOS DEVICE.

(B) MIXING IN DUAL-GATE TRANSDUCER. WITH SIGNAL ON FIRST GATE THE APPLICATION OF A LOCAL OSCILLATOR SIGNAL AT SECOND GATE CAN PRODUCE MIXING IN THE INTEGRATED TRANSDUCER ITSELF AND OUTPUT AT AN INTERMEDIATE FREQUENCY. MAXIMUM SUM OR DIFFERENCE OUTPUT IS OBSERVED WHEN DC SECOND GATE BIAS IS ADJUSTED FOR MAXIMUM RATE OF CHANGE OF TRANSCONDUCTANCE WITH SECOND-GATE BIAS VOLTAGE.

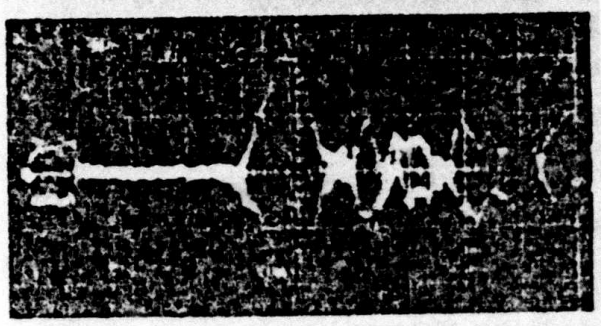

OUTPUT DISPLAYED DIRECTLY (NO LOCAL OSCILLATOR ON SECOND GATE) IN RESPONSE TO 5.5 MHz COMPRESSIONAL WAVE EXCITATION. 1μS/DIV. HORIZONTAL SCALE.

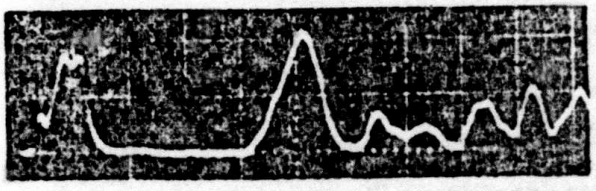

MIXING IN DUAL-GATE TRANSDUCER LOCAL OSCILLATOR 23.8 MHz. OUTPUT OF 30 MHz IF AMPLIFIER WITH DETECTOR.

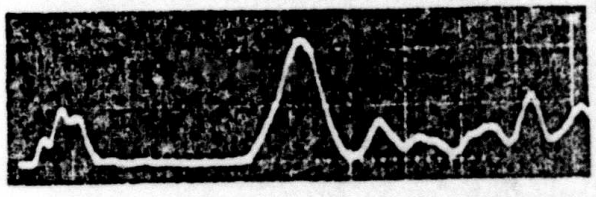

MIXING IN DUAL-GATE TRANSDUCER LOCAL OSCILLATOR 35.2 MHz. OUTPUT OF 30 MHz IF AMPLIFIER WITH DETECTOR.

frequencies.

These frequency translation or mixing properties might be of value in a complex installation for frequency multiplexing of many outputs on a single output cable.

(3) Built-in calibration

It would be easy to incorporate within the FET transducer package a ZnO sending transducer which could be excited occasionally in order to test for any changes in the condition of the transducer, such as disbonding of the transducer from its mounting surface or for gross changes of the gain of the FET. The ZnO calibrating source could be driven by a conventional TTL pulser made in the silicon wafer containing the FET. While the acoustic power output of the thin ZnO is severaly limited by the voltage which it can safely withstand, it should be possible to generate a signal large enough for test of conditions within that one transducer. Source directionality could be exploited for testing differently oriented receiving transducers. Disbonding would in general be indicated by an increase in response to the test pulse, as the acoustic loading of the transducer by the substrate would have been decreased.

(4) Metallic substrate and deposited-in-place transducers

As mentioned in Sec. 1-C, we have successfully deposited ZnO on stainless steel sheets, from 0.002 to 0.020

inches thick, obtaining deposits which are oriented fairly well (x-ray rocking angle curves have a spread of $\pm 3.5^{o}$). Transducers based on such a material and having FET dies bonded onto them could be used for continuous monitoring in structures. We have punched mounting holes in the coated sheets and flexed the sheets without causing any cracking or flaking of the ten micron thick ZnO films.

We have also found that one can make electrochemically deposited ZnO films which are piezoelectric. Graduate student Jon Bernstein (1980) has shown that anodically oxidized metallic zinc films showed response to bulk longitudinal waves in a test at 10 MHz. Though this work is in an early stage, it does suggest the intriguing possibility that one could deposit transducing films directly onto structures quickly, either during production of parts, or afterwards by using a small cup sealed temporarily to the surface of the part and within which electroplating and anodization takes place.

1-F: Summary of present state of development

The ZnO-FET transducer is in the laboratory stage at this time. Much work has been done on it and most of its features are identified and well understood.

To take this device to the field model stage requires identification of a specific application, such as the acoustic emission application defined by Battelle. For example,

two options for obtaining higher sensitivity have been outlined above; if more sensitivity is desired, those options could be pursued. What directional characteristics are desired? Once that question is answered, the transducer electrodes can be designed to provide those characteristics.

If this promising device is to be developed for the acoustic emission application envisioned, it is important that there be close contact among University personnel, Battelle personnel, and the ultimate user. In short, the greatest rate of progress will result when the real problem -- the application -- is clearly defined.

To give some idea of how this device might appear in a field model, Fig. 1-13 shows at top a hybrid ZnO-FET transducer in a small housing with two miniature coaxial cables to provide for bias and signal output. The lower photo shows a ZnO transducer deposited on a thin stainless steel sheet and connected via the miniature coaxial cable to an external amplifier. Finally, Fig. 1-14 compares outputs, in response to a pulse from a shock-excited 10 MHz commercial ultrasonic transmitting transducer, of a commercial broadband NDT transducer (a) and ZnO on a 0.002 inch thick stainless steel sheet (b).

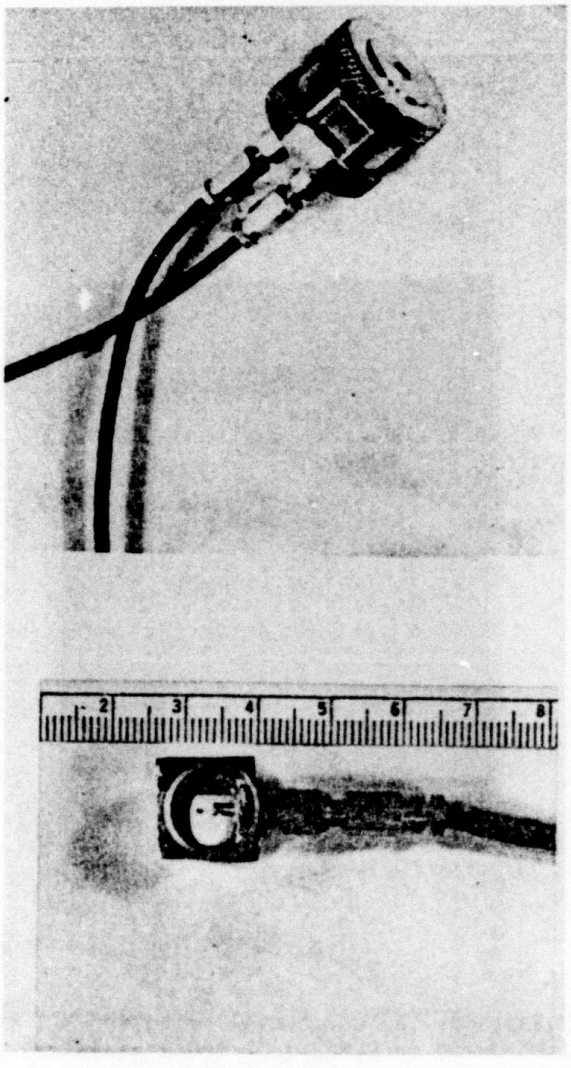

Figure 1-13. Zinc Oxide Transducers.

Top: Transducer housing containing ZnO film on small die protruding from broad face of brass enclosure. Die containing commercial DMOS transistor is inside brass housing. Miniature coaxial leads supply bias current and provides for signal output.

Bottom: ZnO on stainless steel sheet (square seen protruding around edges of brass tubing which forms housing). Electrode on ZnO is the bright circle, and is connected to coaxial output. Scale in centimeters.

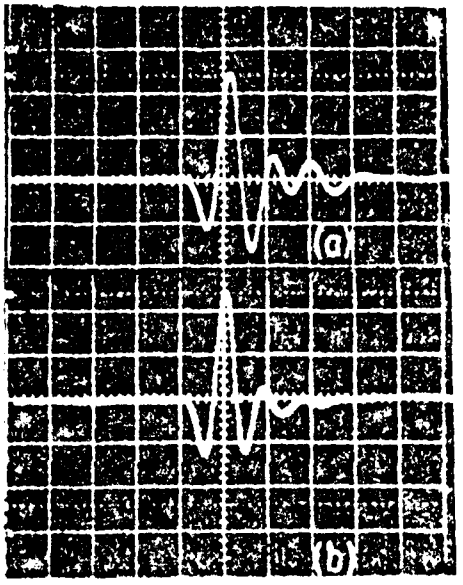

Figure 1-14. Outputs of (a) commercial broadband NDT transducer and (b) zinc oxide on 0.002-inch thick stainless steel, in response to pulse from commercial NDT transducer with a plexiglass cylindrical block as delay medium. Vertical scale: arbitrary; horizontal: 100 nanoseconds/division.

REFERENCES

Bernstein, J. J., 1980, Master of Science Report, U. of California, Berkeley.

Callerame et al., 1979, Proc. IEEE Ultrasonics Symposium, p. 407.

Chuang et al., 1979a, Proc. IEEE Ultrasonics Symposium, p. 915.

Chuang et al., 1979b, Proc. IEEE Ultrasonics Symposium, p. 114.

Kwan, S. H., 1978, Doctoral Dissertation, U. of California, Berkeley.

Kwan et al., 1979, IEEE Trans. Elec. Dev., ED-26, p. 1053.

Muller and Conragen, 1965, IEEE Trans. Elec. Dev., ED-12, pl 590.

Shiosaki, 1978, Proc. IEEE Ultrasonics Symposium, p. 100.

White et al., 1980, preprint of submission to IEEE Trans. Sonics Ultrasonics.

Yeh and Muller, 1976, Appl. Phys. Lett., Vol. 29, No. 9, p. 521.

APPENDIX E

NBS POINT DISPLACEMENT SENSOR

T. Proctor
D. Eitzen
National Bureau of Standards

NBS Point Displacement Sensor
T. Proctor and D. Eitzen

Section 1. Present Status

(a) Physical Principles.

The device is a pzt-type sensor which has been designed to be essentially free of internal mechanical resonances and internal acoustical reflections, within the range of frequencies of interest. The other significant design feature is the very small contact area. This avoids the distributed area interference effects associated with transducers which have large diameters compared to a wavelength at the frequencies of interest. As a result these transducers are point receivers. The absence of a wear plate on the transducer front avoids interference effects associated with the wear plate thickness. The transducer faithfully reproduces the normal surface displacement at a point.

Figures 1 through 4 are the standard results of the comparison calibration technique used at NBS. Figures 1 and 2 are the time wave forms of the capacitance standard transducer and of the improved piezoelectric transducer briefly described above. Except for a small undershoot this transducer reproduces the step force function Rayleigh wave. Note that the NBS Point Displacement Sensor measures the normal displacement of the surface almost as accurately as the standard capacitive transducer (known to measure absolute displacement within a few percent) and with much more sensitivity. Figure 3 is the displacement response of the improved transducer. Note the ordinate is a linear scale which accentuates variations as compared to the log scale normally used. Figure 4 gives the phase response of the transducer. No sudden changes occur in phase as a function of frequency.

(b) Sensitivity.

It is very difficult to describe acoustic emission (AE) transducers by longitudinal, shear and surface wave sensitivities. In order to measure such sensitivities one needs a pure source of the particular transmittal mode. This requires that the transducer be set up on the axis of its pure mode generator; but because of the unknown location of the AE event, a mixture mode will normally excite the transducer. This situation is further complicated because usually the structure for AE investigation has a great variety of shapes and dimensions. This gives rise to multiple reflection paths, and with mode conversion on reflection, the chances of the received signal being a mixture of all modes of motion is guaranteed. As a result, it is more convenient and illuminating to talk about sensitivity to horizontal and vertical motion of the mounting surface. It is for this reason that we do our calibrations on the big steel block and relate the sensitivity to the horizontal and vertical displacement associated with the surface Rayleigh wave. In these reference terms the vertical component sensitivity of displacement for some typical NBS point sensors is about 1×10^8 v/m. This is a displacement sensitivity and is unamplified. By design, the horizontal sensitivity is minimal.

(c) Bandwidth and Sensitivity.

These improved transducers have a bandwidth which is greater than 1 MHz. These transducers are essentially free of any resonances in the range of 50 kHz to at least 1 mHz. The response can best be described by a slight increase in vertical displacement sensitivity over this range in frequencies. This increase amounts to about 1.7 times in amplitude over the range of 200 kHz to 1 mHz; small variations in sensitivity along this nearly monotonic increasing function amount to less than 30% (see fig. 3). Phase response is also a critical consideration as it adds information to processing such as

Fourier transformation that one might perform. Thus transducer phase reproduction is important. In general tranducers which have resonances in their spectra also have abrupt phase rotation of the electrical output at these frequencies of resonance. The NBS point transducers have very well behaved phase response curves which improves the chances of getting meaningful FFT transformation (See Fig. 4).

Another test of the fidelity of the transduction is simply the ability to respond to the known displacement. Fig. 1 shows actual surface displacement as measured by the capacitive transducer and Fig. 2 is the response as measured by the NBS point transducer.

(d) Beam Characteristics

As receivers these transducers should perform much like point receivers and show little or no directional sensitivity. However, for an AE transducer any directional considerations are clouded by the complex geometry of the AE medium that produces many different paths for energy to arrive at the receiver. Thus the effects of some specific directionality sometimes become difficult to evaluate. But, in short, the NBS point sensor has the fortunate characteristic of essentially no directionality.

(e) Stage of Development

The NBS improved transducers are in the prototype stage. Sufficient numbers have been made and used to assure usefulness in a laboratory environment. Their behavior is not fully described and their long-term stability is not fully known.

Section 2. Development Required to Provide Several Working Models

To advance to the working model stage requires an evaluation of

reliability and stability of these transducers. Some improvement in the response characteristics and sensitivity may be achieved by an in depth analysis of their mechanical and acoustical behavior which we propose to do. A small integrated preamp will be designed to overcome the effects of capacitance loading on the transducer signal. Mechanical attachments to the agreed upon test specimen will also be designed. Three working transducers with matching preamps will be constructed and initially calibrated.

(a) Time and Cost.

Three to five working transducers could be supplied within a few months. If calibration of these transducers were required, this time frame would be lengthened somewhat. A longer time period would be required to run the stability and reliability evaluation. The more complete analysis of transducer behavior is also a longer-term involvement.

To supply the working prototypes and solve the problems of shielding, transducer mounting and electronic matching will require about a half man-year effort. The longer term efforts of understanding the transducer stability and reliability and a more complete analysis would require another half man-year effort.

(b) Supporting Equipment.

The proposed project will be accomplished with the equipment, electronic and mechanical, and with the tools presently available here at NBS.

(c) Bandwidth and Sensitivity.

Bandwidth and sensitivity that can be expected of the delivered working models will be equal to or better than that of the present prototypes.

Figure 5 shows a comparison of the spectral response of a typical NBS Point Displacement Sensor with the Battelle M-13 transducer. The solid line is the displacement response of the NBS improved transducers. The dashed line is the displacement response of the Battelle M-13 transducer. Figure 6 is a comparison of phase response for the same two transducers. Both measurements were made using the NBS Calibration set up and the displacement response is relative to 1 volt per μ meter on the dB scale.

Section 3. Development of Field Model

It is nearly impossible to estimate such factors of cost and time to produce a working field transducer without knowing more about the environment under which they will work. Questions of temperature, pressure, static and dynamic electric background field, g-forces, etc. need to be known if any reasonably realistic estimate can be made. However, the NBS point type tranducer is similar in basic construction to commercially available transducers and would therefore have about the same chance to be developed to fit in and perform in the environment in an aircraft.

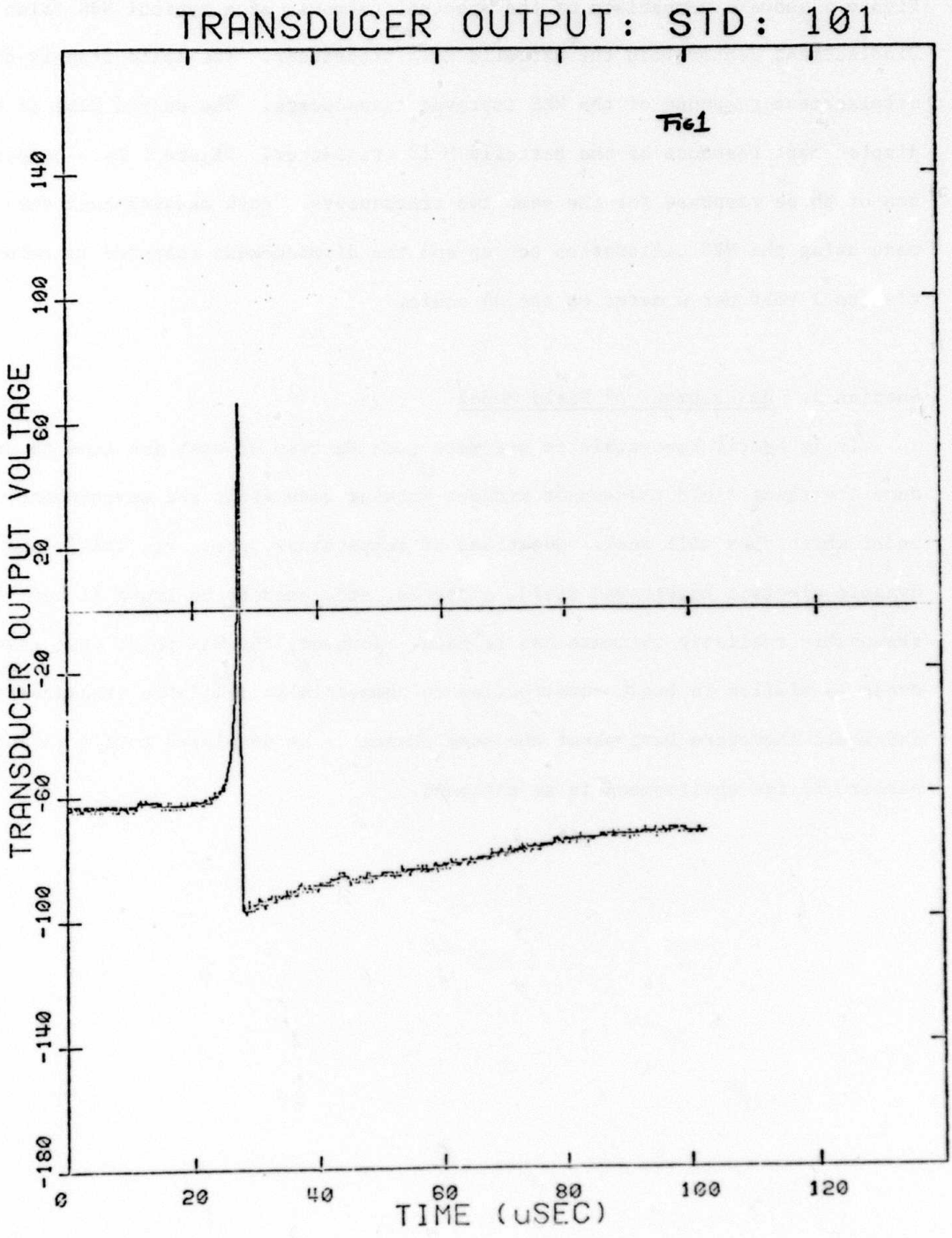
TRANSDUCER OUTPUT: STD: 101
Fig1
TRANSDUCER OUTPUT VOLTAGE
140
100
60
20
-20
-60
-100
-140
-180
0
20
40
60
80
100
120
TIME (uSEC)

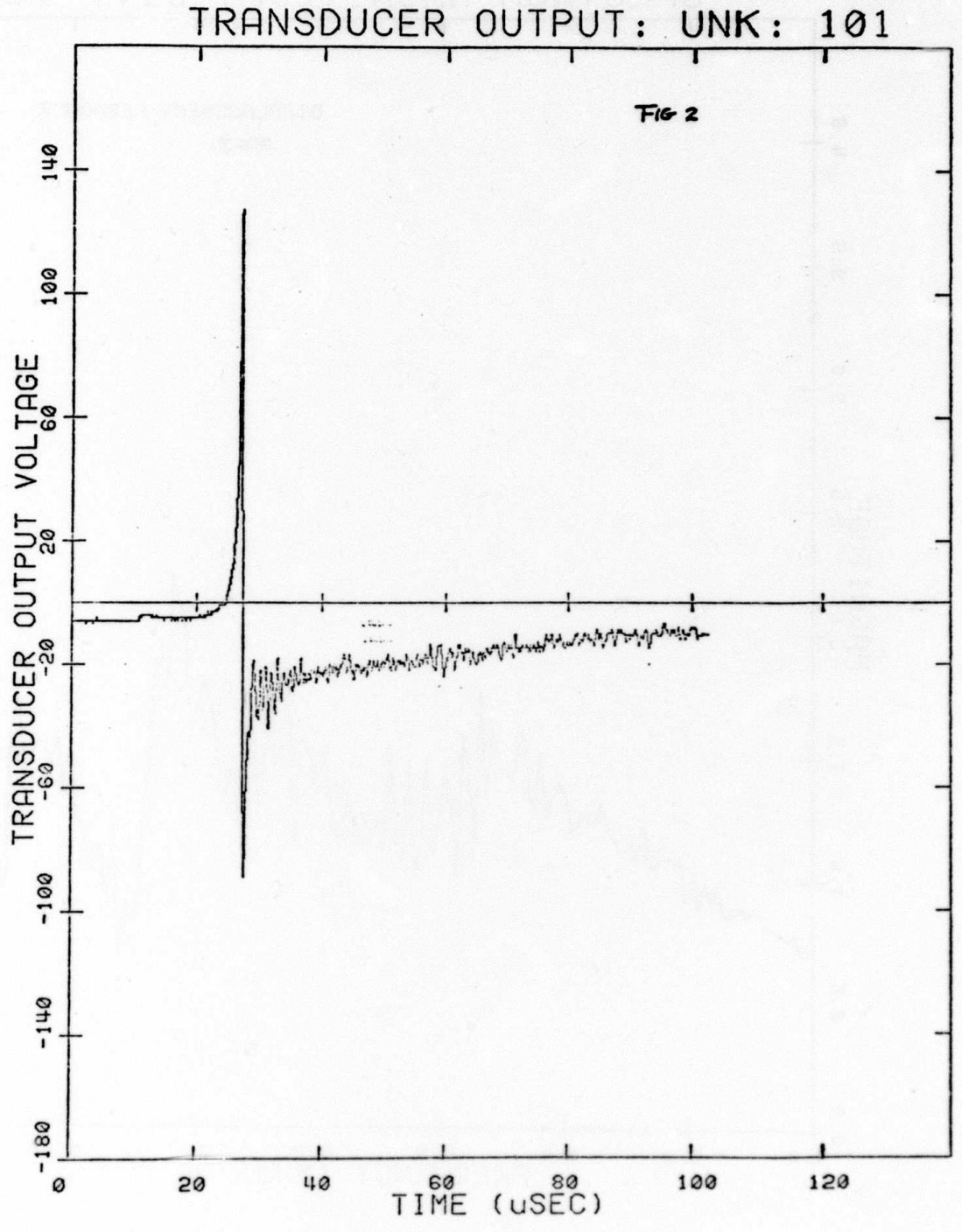
TRANSDUCER OUTPUT: UNK: 101
FIG 2
TRANSDUCER OUTPUT VOLTAGE
140
100
60
20
-20
-60
-100
-140
-180
0
20
40
60
80
100
120
TIME (uSEC)

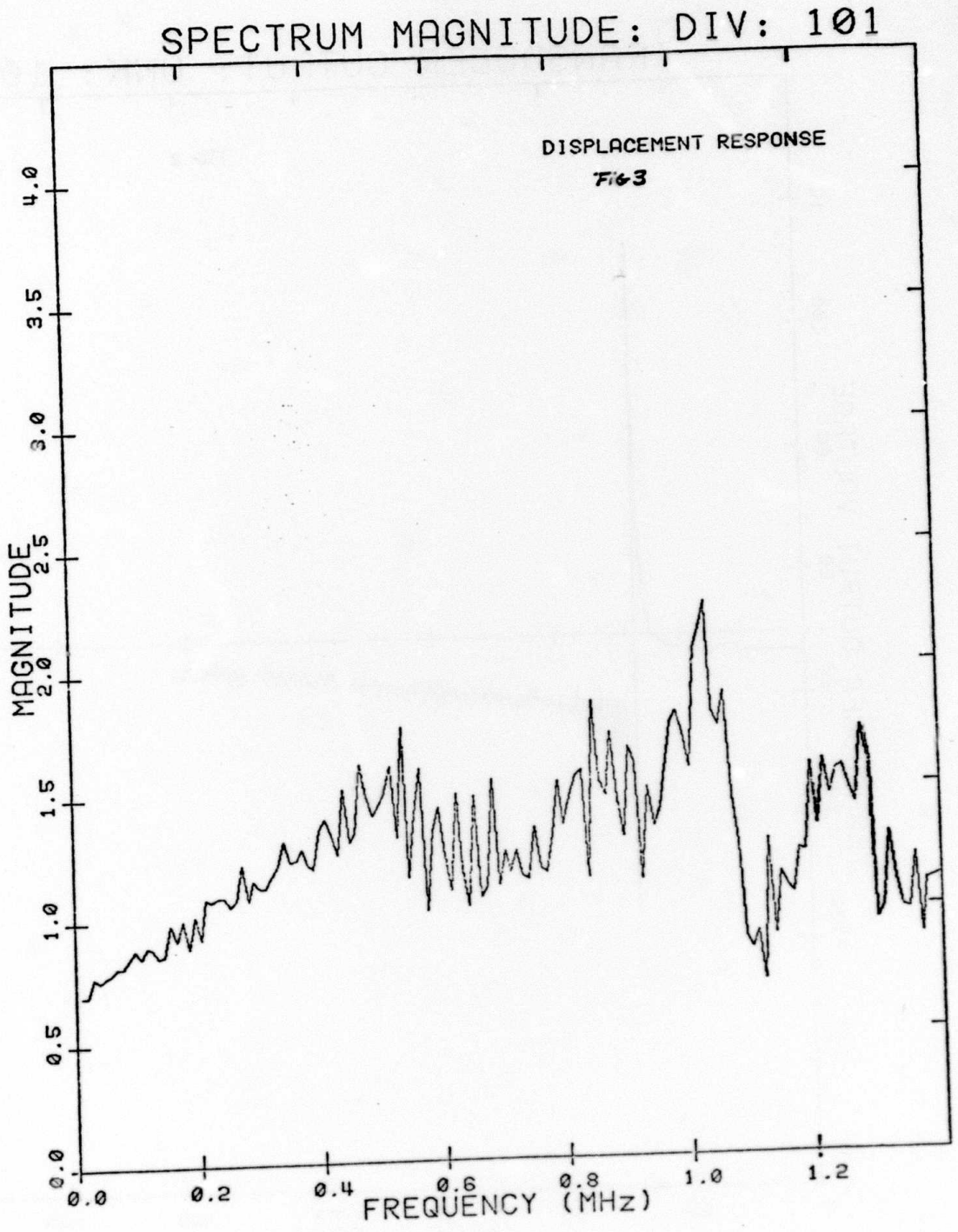
SPECTRUM MAGNITUDE: DIV: 101
DISPLACEMENT RESPONSE
FIG3
MAGNITUDE
0.0
0.5
1.0
1.5
2.0
2.5
3.0
3.5
4.0
0.0
0.2
0.4
0.6
0.8
1.0
1.2
FREQUENCY (MHz)

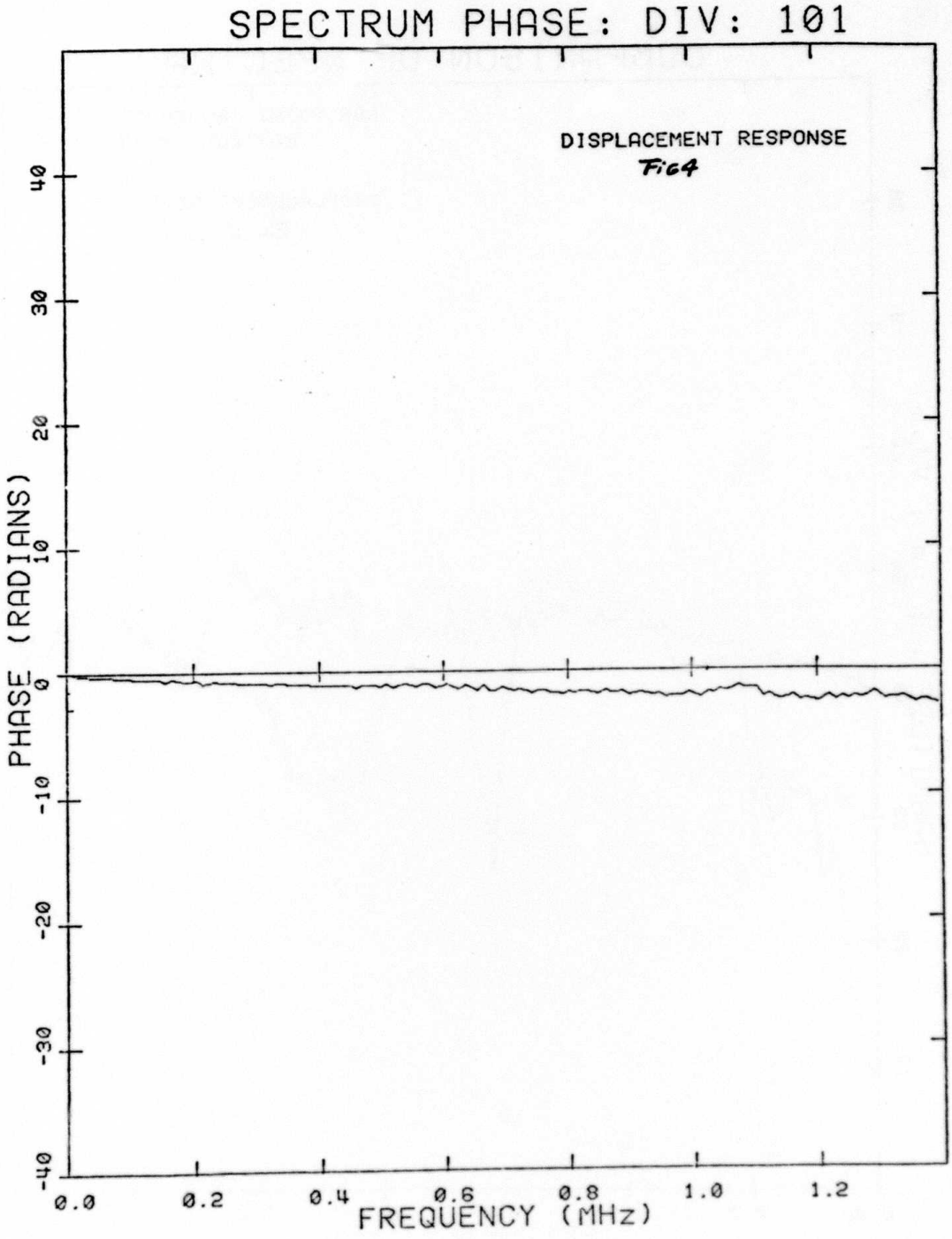
SPECTRUM PHASE: DIV: 101
DISPLACEMENT RESPONSE
Fig4
PHASE (RADIANS)
40
30
20
10
0
-10
-20
-30
-40
0.0
0.2
0.4
0.6
0.8
1.0
1.2
FREQUENCY (MHz)

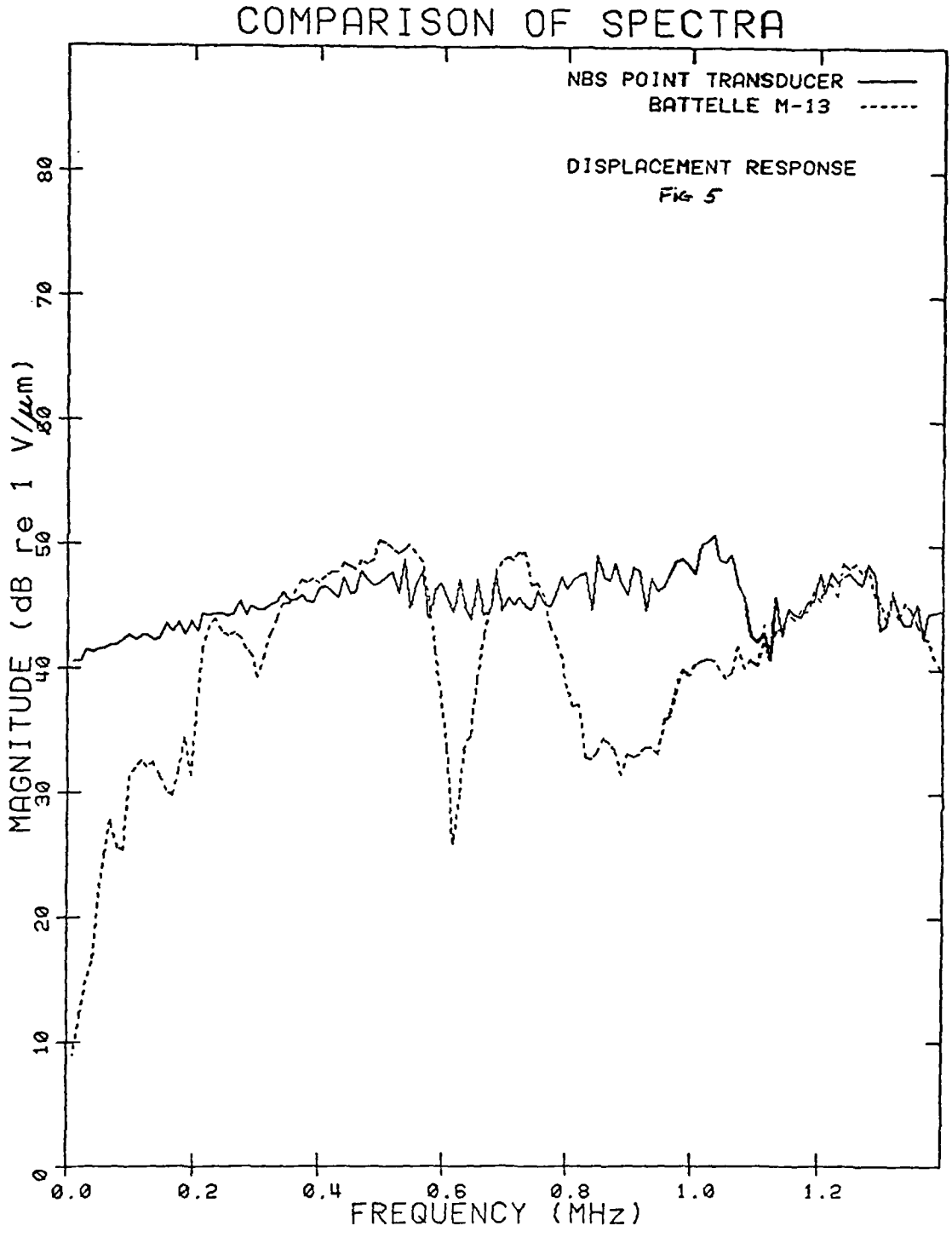
COMPARISON OF SPECTRA
NBS POINT TRANSDUCER
BATTELLE M-13
DISPLACEMENT RESPONSE
FIG 5
MAGNITUDE (dB re 1 V/μm)
0
10
20
30
40
50
60
70
80
0.0
0.2
0.4
0.6
0.8
1.0
1.2
FREQUENCY (MHz)

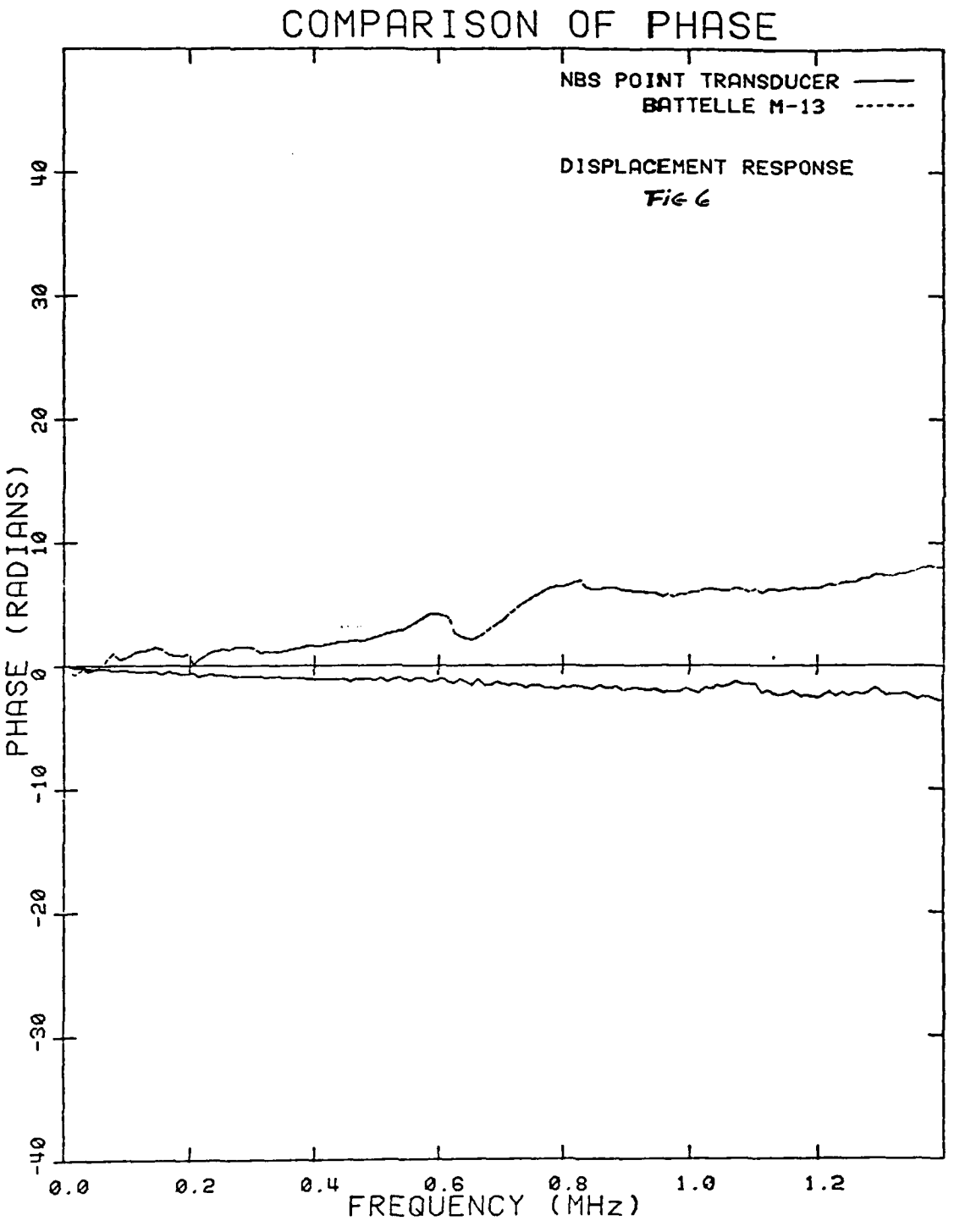
COMPARISON OF PHASE
NBS POINT TRANSDUCER
BATTELLE M-13
DISPLACEMENT RESPONSE
Fig 6
PHASE (RADIANS)
40
30
20
10
0
-10
-20
-30
-40
0.0
0.2
0.4
0.6
0.8
1.0
1.2
FREQUENCY (MHz)

APPENDIX F

POLYVINYLIDENE FLOURIDE TRANSDUCERS AS ACOUSTIC EMISSION SENSORS

W. R. SCOTT
Naval Air Development Center

POLYVINYLIDENE FLUORIDE TRANSDUCERS AS ACOUSTIC EMISSION SENSORS

W. R. SCOTT

NAVAL AIR DEVELOPMENT CENTER
WARMINSTER, PENNSYLVANIA 18974

POLYVINYLIDENE FLUORIDE TRANSDUCERS AS ACOUSTIC EMISSION SENSORS

I. A. INTRODUCTION

Polyvinylidene fluoride is a piezoelectric crystalline polymer (> 40% crystallinity) with the structural formula shown in Figure 1. Although the material can exist in a number of phases or crystal structures with this same structural formula only one of these phases (planar -zigzag, designated β) is readily polarized, the overall percentage and the orientation of this phase determining the strength and directionality of the piezoelectric properties for the material.

The phase transformations and crystalline reorientations which take place during fabrication and poling of the material are the principal mechanisms which may be used to control the directional properties of PVF_2.

B. SENSITIVITY AND FREQUENCY RESPONSE

There is no general straightforward way of defining sensitivity for a piezoelectric material, since incorporation into devices always produces properties which are to some extent determined by boundary conditions, geometry and frequency. However, two piezoelectric constants which are ordinarily used to determine sensitivity of such materials are the g constant (proportional to the open circuit voltage produced for a given applied stress and the h constant (proportional to the open circuit voltage produced for a given strain). At present, reliable measurements of g and h are not available for PVF_2 as a function of frequency and crystal orientation; however, reasonable estimates of dynamic sensitivity may be obtained from D.C. measurements. These give a unidirectional g value (g_{13}) of 200 V m/N for PVF_2 as compared to 90 V m/N for Rochelle salt, 50 V m/N for quartz and 10 V m^2/N for PZT. On the other hand the h value for PVF_2 is about 60 V/m as compared to 95 V/m for PZT. 390 V/m for quartz and 340 V/m for Rochelle salt.

Clearly, the most sensitive material for use in a given piezoelectric device is dependent on how the excitation to be detected is coupled to the transducer. If PVF_2 material is used like a strain gage (i.e., following the deformation of a high impedance material) it will be relatively insensitive as compared to ceramic materials. If, however, the material is used in such a manner that it restricts for example a thickness mode of excitation, either through clamping or inertial pinning, then the high compliance of the PVF_2 will permit large deformations to take place resulting in higher sensitivity that can be obtained with other materials.

Experimentally, Scott and Carlyle[1] found that PVF_2 transducers of 25 μ thickness exhibited (by a factor of two or more) larger responses for narrow broadband pulses (width less than .5μ) than did several commercial AE and ultrasonic pulse echo transducers. These results were obtained from tests in which the thin PVF_2 element was clamped between a commercial transducer to which it was being compared and a medium in which an excitation was propagated.

[1] W. R. Scott and J. M. Carlyle "Acoustic Emission Signature Analysis" NADC Report No. 3930-1, p. 115 July 1975.

In the above experiments signals were amplified using relatively high impedance (< 20 kΩ) providing relatively low electrical damping of the piezoelectric detector. Under these conditions the PVF_2 device exhibited virtually no ringing as compared to commercial broadband devices which continued to ring for up to milliseconds. Similar results confirming the broadband characteristics of PVF_2 were reported by Bui, Shaw and Zitelli[2] who measured an essentially flat frequency response for the material between 1 and 20 MHz. Of course, frequency response for a device incorporating PVF_2 will always exhibit features associated with other elements of the device and resonances occurrring in unclamped backing material or wear plates will be seen in the output of the device.

Since the art of transducer design as currently practiced generally incorporates piezoelectric elements having a low damping and relatively high acoustic impedance, velocity of sound and density (the exact opposite of PVF_2) the optimum utilization of this material as an ultrasonic sensor will require careful reexamination of fundamental design assumptions.

C. BEAM CHARACTERISTICS AND DIRECTIONALITY

Because polyvinylidene fluoride is a "crystalline" polymer its piezoelectric properties are quite anisotropic and dependent upon the manner in which the material is fabricated. Material which is unidirectionally stretched (in the plane of the film) will generally have a value of g_{31} (where 1 is the stretching direction and 3 is the through thickness direction) ten times larger than g_{32} (2 being perpendicular to 1 and 3).

For acoustic emission application it would be desirable to utilize the high g constant of the material $g_{31} \approx 200$, $g_{hydrostatic} \approx 60$, and this could produce a very directional device.

Recently, EMI has reported the fabrication of a PVF_2 material with a $g_{hydrostatic} > 200$, which would be expected to have good sensitivity for longitudinal waves traveling in any direction; however, considerable directionality is still likely. Also the fabrication of devices from bundles of oriented piezopolymer fibers has been considered by Hudemac[3] and others. Such devices would undoubtedly be more controllable in uniformity of sensitivity but are not likely to be available in the near future.

Very little has been reported on the sensitivity to shear waves of the PVF_2 film which is currently available. In order to reliably assess the sensitivity of PVF_2 to such waves, measurements should be made of the constants g_{14}, g_{15}, g_{16}, g_{24}, g_{25}, g_{26}, g_{34}, g_{35}, and g_{36} for the materials currently available.

[2] L. Bui, H. H. Shaw, and T. Zitelli "Experimental Broadband Ultrasonic Transducers Using PVF_2 Piezoelectric Film" Ginzton Laboratories. Report No. 2573.

[3] Hudemac, A. A. JASA, 66(2) August 1979, p. 556

E. STATE OF DEVELOPMENT

At present the capability for fabricating a PVF_2 passive device for acoustic application exists in several laboratories in this country including Ginzton Laboratories, Stanford, Naval Air Development Center and National Bureau of Standards; however, there has been no concerted effort directed toward optimizing or packaging such a device. Studies by Scott and Carlyle[4] demonstrated that adequately shielded but unbacked PVF_2 devices could be used for monitoring acoustic emission from samples of titanium and graphite/epoxy and the unoptimized devices used in these studies provided sensitivities comparable to commercial acoustic emission transducers but with much wider bandwidths.

Basic considerations indicate that mass loading such devices would have increased their sensitivity, at least at low frequencies, and currently available material should have higher activity than that used in the earlier studies.

II. DEVELOPMENT REQUIRED TO PROVIDE WORKING MODELS

On the basis of theoretical considerations and the experimental work described above, it appears reasonable to expect that a PVF_2 acoustic emission transducer could be constructed having a broadband longitudinal mode sensitivity between 2 and 20 times greater than could be achieved with other piezoelectric materials, although the potential advantages of lightweight and flexibility would possibly be sacrificed in packaging in order to obtain sufficient inertial mass and adequate electrical shielding. The low noise benefits of using a remote preamplifier attached to the transducer would be much the same here as for any piezoelectric transducer and this option should be considered if remote powering of the transducer package is possible.

A modest analysis effort aimed at optimizing transducer design ($\lesssim$ 55K) should be undertaken once a decision has been made as to desired size, shape and frequency response of the device and the type of waves it is desired to detect.

Since reliable g constants needed to determine shear wave sensitivity of PVF_2 are not available, these should be measured (> 40K study) in order to have a quantitative predicition of transducer sensitivity for such waves. In any case, mode conversion would provide reasonable sensitivity for all but normal incidence shear waves even if these g values were low

The best material available currently for the above studies is probably that manufactured by EMI, England although its cost ($\sim$ \$100/sq. in.) is one or two orders of magnitude higher than material available from other sources. If this supplier is selected material costs could run to \$20K or more depending on the size and number of devices to be tested and the amount of material characterization desired.

[4] W. R. Scott and J. M. Carlyle "Acoustic Emission Signature Analysis" Report IR Task No. ZR01108 (1976) p. 25.

The laboratory construction of a few optimized PVF_2 devices with the accompanying electronics packages should cost about $40K for the first unit and about $3K per copy thereafter.

III. CONSIDERATIONS FOR FIELD MODELS

There is nothing intrinsically different or more expensive about fabricating PVF_2 devices than any other piezoelectric device once the initial design parameters are established; hence, such a device should cost no more and be no larger than a PZT or quartz device of comparable sophistication.

The mechanical ruggedness of such a device, when it is properly packaged, should exceed that of any ceramic transducer, but the thermal environment must be controlled since prolonged exposure of the device above $140^{\circ}F$ may produce deformation of the PVF_2 and loss of piezoelectric activity.

Exclusive of any remote preamplification capability a commercial manufacturer should be able to supply PVF_2 devices at less than $600/copy.

Figure 1. Structural Formula of Polyvinylidene Fluoride

APPENDIX G

Broadband Acoustic Emission Transducers

G. S. Kino
Stanford University

BROADBAND ACOUSTIC EMISSION TRANSDUCERS

G. S. Kino

Abstract

A study has been made of acoustic emission transducers for operation in the frequency range from 100 KHz to 2 MHz . We consider the basic design required for receiving both Rayleigh waves and longitudinal waves incident on the transdsucer over a wide angular range. Various types of piezoelectric transducers, the capacitor transducer, the fiber optic transducer, acousto-electric transducers, and array transducers are considered. We conclude that a conventional PZT 5H contacting transducer of approximately 1 mm diameter is the best choice for an acoustic emission detector operating from 100 KHz to 2 MHz .

BROADBAND ACOUSTIC EMISSION TRANSDUCERS

G. S. Kino

I. INTRODUCTION

The design of acoustic transducers for use in acoustic emission testing has mainly followed the methods used for NDE transducers. The minor changes in design usually made for this purpose mainly concentrate on the facts that the frequency of operation is typically below 400 KHz , and that an omni-directional sensor is required. In addition, because of the often difficult working environment, a great deal of attention has to be paid to the need to differentiate against interfering signals.

We shall consider here the design problem for AE (acoustic emission) transducers to operate over a broad band in the range from 100 KHz - 2 MHz . We shall be concerned with transducers that can respond to Rayleigh waves, longitudinal waves, and shear waves. We shall consider the use of standard piezoelectric transducer ceramic materials and also non-standard materials such as ZnO thin films, PVF_2 plastic, and composites. New concepts such as the use of fiber optics and acoustoelectric transducers are also of interest and will be considered.

II. BASIC NEEDS FOR ACOUSTIC EMISSION TRANSDUCERS

Pao[1] has discussed simple types of AE sources. In his terms, a small crack opening up or grain boundary cracking could

be regarded as a double force source, a single couple, or a double couple without movement. In each case, if the force has a frequency spectrum f_ω, it can be shown that there are radiated displacement amplitude components from a buried source of the form $\omega f_\omega(\exp - jkR)/R$ where $k = \omega/v$ is associated with a propagating shear or longitudinal wave, and ω is the radian frequency. As a typical source corresponds to a step function release in stress, f_ω varies as $1/\omega$. Thus the displacement amplitude from a small source of this type should be uniform over the frequency range of interest.

The situation becomes more complicated for finite crack sizes because of crack resonances and Rayleigh wave propagation along the crack surface and Doppler shifts associated with moving crack fronts. Furthermore, when the wave guiding properties of the structure itself are taken into account, the situation changes. For instance, a surface crack will emit a surface wave signal that falls off as $\exp -jk_R R/\sqrt{R}$ where k_R is the Rayleigh wave propagation constant. Therefore the surface wave excitation tends to become dominant at some distance from the exciting source and its frequency dependence different from that of a bulk wave. It is apparent that the frequency distortion will be even more severe when multiple Lamb modes are excited. At all events, at short distances from the flaw, a detector on the surface of a structure will tend to observe all possible modes that are excited by AE sources. At longer distances from the source, if the source is within a Rayleigh wavelength from the surface, acoustic surface wave signals may well be dominant

at the detector. On the other hand with a buried AE source, only bulk waves will tend to be present, unless there is some conversion to surface waves at sharp corners.

Thus the basic transducer must be able to detect normal displacements of the surface of the structure. In principle, this will make it possible to detect longitudinal waves and surface waves, both of which have such displacements present. A shear wave arriving at an angle to the surface normal will also excite such a transducer. But a shear wave source directly underneath the transducer would only give rise to a displacement parallel to the surface, which would have to be detected by a shear wave transducer. This is a relatively rare case, so we will in the main, concentrate on transducers capable of detecting displacements normal to the surface.

Since we do not normally know the position of the emission source beforehand, it is appropriate to design an omni-directional transducer capable of detecting bulk waves or surface waves. In a few cases where the position of the possible source is known, such as a crack in a particular bolt hole, it may be appropriate to design to receive surface wave or bulk wave signals from a particular position. This makes the task easier. We will therefore address ourselves only to the problem of design of an omni-directional broadband 100 KHz - 2 MHz transducer. If this can be solved well, the design of other narrower band, narrower acceptance angle transducers should not be a major problem.

III. THE DIAMETER OF A BROADBAND TRANSDUCER

Suppose we wish to design a transducer to detect a surface wave of propagation constant k_R propagating at an arbitrary angle ϕ to the x axis as shown in Fig. 1. The transducer is supposed to detect the normal displacement u_z of the surface, and we can write

$$u_z = u_0 e^{-jk_R(x \cos \phi + y \sin \phi)} \tag{1}$$

A piezoelectric, fiber optic, or capacitive transducer placed in contact with the surface basically responds to the average value of u_z over the area of the transducer. Hence, in order to make the response independent of ϕ, the transducer must be cylindrical in shape of radius a. In this case, its response will be of the form

$$V = \frac{1}{\pi a^2} \int e^{-jk_R(x \cos \phi + y \sin \phi)} \, dxdy \tag{2}$$

writing $x = r \cos \phi'$, $y = r \sin \phi'$

$$V = \frac{1}{\pi a^2} \int_0^a \int_0^{2\pi} re^{-jk_R r \cos(\phi' - \phi)} \, d\phi' dr \tag{3}$$

This integral can be shown to give the result

$$V = \frac{2J_1(k_R a)}{k_R a} \tag{4}$$

where $J_1(x)$ is a Bessel function of the first kind and first

order with its first zero at $k_R a = 3.83$. The 3 dB points of this function are where

$$\left(\frac{a}{\lambda_R}\right)_{3\ dB} = 0.24 \tag{5}$$

On the other hand, it can be shown from the work of Ref. 2 that if we consider a longitudinal wave of wavelength λ_L amplitude u_0 incident on the transducer at an angle θ to the normal, it has an amplitude $u_z = u_0 \cos\theta \exp -jk_L x \sin\theta$ normal to the surface, as illustrated in Fig. 2. Thus at the surface, the effective response varies as

$$\Phi = 2 \cos\theta \frac{J_1(k_\ell a \sin\theta)}{k_\ell a \sin\theta} \tag{6}$$

It follows that because of the $\cos\theta$ term, under no circumstances can the transducer respond to longitudinal waves arriving at an angle nearly 90° to the normal.

If we use the requirement of Eq. (5) and take $k_\ell \approx 0.5\ k_R$ as is typical for most material, we observe that the 3 dB points for Rayleigh waves gives $k_\ell a \approx 0.12$. Hence the transducer will have its 3 dB longitudinal wave angular response points close to ±45° .

It will be observed that this requirement is a severe one, which it is tempting to relax. For a transducer operating up to a frequency of 2 MHz with typical metals ($V_R \sim 3 \times 10^5$ cm/sec) , Eq. (5) implies that the diameter must be less than 0.75 mm . Even for a transducer operating only up

to a frequency of 400 KHz , the requirement is for a diameter of the order of 4 mm .

As we shall see, piezoelectric transducers respond to the rf velocity rather than displacement, i.e. ωu . Hence for this reason the response to emission tends to increase with frequency. Therefore it may be appropriate to work with a larger transducer than is indicated by this result. Nevertheless, if we still require a good angular response function, it follows from Eq. (6) that it is necessary to keep the diameter small, and the slight relaxation of our requirements for Rayleigh waves can only result in increasing the diameter to perhaps 1 mm . We shall consider in our design a transducer of this diameter. We shall also consider other types of larger diameter transducers for operation at lower frequencies.

IV. IMPEDANCE MISMATCH FOR VARIOUS TYPES OF TRANSDUCERS

We shall consider first a transdsucer operating into an extremely high impedance load, i.e. an open circuited transducer. Later we shall consider the effect of a capacitive load.

We shall consider the transducer to be in contact with the surface. We shall be concerned with excitation of a longitudinal wave approaching the transducer at normal incidence to the transducer. Thus the stress reflection coefficient of the incident wave is

$$\Gamma = \frac{Z_L - Z_1}{Z_L + Z_1} \tag{7}$$

where Z_1 is the impedance of the substrate and Z_L the impedance presented by the transducer.

The velocity transmission coefficient is

$$T = \frac{v_1}{v^+} = 1 - \Gamma = \frac{2Z_1}{Z_L + Z_1} \tag{8}$$

where v_1 is the input velocity at the transducer surface and v^+ the velocity amplitude of the wave traveling toward the surface as illustrated in Fig. 3.

It is not as simple to calculate the reflection coefficient of a Rayleigh wave. However, we can make a reasonable estimate of the excitation by making use of the results for excitation of waves in a solid by a piston transducer. It has been shown that when a piston transducer, excited with a longitudinal wave, is placed in contact with a solid, the transducer excites longitudinal, shear, and Rayleigh waves in the solid.[2,3] The effective impedance presented to the transducer is Z_1'. The theory has been calculated in detail for an infinitely long rectangular transducer and a piston transducer placed in contact with a solid.[2,3] The result of the calculation showed that $Z_1' \approx Z_1$ the longitudinal wave impedance if the width of the transducer is greater than $\lambda_L/2$ in the solid substrate. Otherwise Z_1' has a reactive component with $\mathrm{Re}Z_1' < Z_1$.

We shall suppose that the total velocity normal to the transducer surface is

$$v_1 = v_R^+ + v^- \tag{9}$$

where v^- is the wave excited in the substrate and v_R^+ the rf velocity of the Rayleigh wave.

We are essentially assuming a sliding contact so that the longitudinal stress at the transducer is

$$T = -v_1 Z_L \tag{10}$$

But this stress excites waves in the substrate, with

$$T = v^- Z_1' \tag{11}$$

It follows that

$$v_1 \left(1 + \frac{Z_L}{Z_1'}\right) = v_R^+ \tag{12}$$

or

$$v_1 = \frac{Z_1'}{Z_L + Z_1'} v_R^+ \tag{13}$$

with

$$v^- = -\frac{Z_L}{Z_L + Z_1'} v_R^+ \tag{14}$$

It will be seen that the dependence of v_1 on v_R^+ is of just the same form as that of Eq. (8). For our purposes, in order to make estimates of efficiency we shall assume that $Z_1' = Z_1$.

V. THE THEORETICAL RESPONSE CHARACTERISTICS OF VARIOUS TYPES OF TRANSDUCERS

We shall initially consider the individual transducers of interest to be terminated by an infinite electrical impedance,

where appropriate. Later we shall concern ourselves with this assumption and show that for many types of transducers of the small size required for our purposes, the capacity of the transducer is so small that this assumption cannot be justified in practice.

For simplicity, we will consider only the response of a transducer to a normally incident longitudinal wave. However, by taking account of the angular response characteristic using Eq. (6) and by taking account of the Rayleigh wave response characteristic using Eqs. (4) and (13), it is possible to change the estimates made in this theory by factors of 2 or so to take account of these effects.

A. The Capacitor Transducer

We suppose that the transducer consists of a metal electrode spaced by a distance ℓ from the surface of the structure. The space is normally taken to be a thin airgap. Thus the acoustic impedance of the transducer is essentially zero, providing the support structure does not interfere with the incident wave.

An alternatiave structures uses a high dielectric constant unpoled ceramic material of the type employed for the capacitive transducer. This would present a finite acoustic impedance to the incident wave which could be estimated in the same manner as we shall do for piezoelectric transducers. In this case, the transducer would have to have a rigid backing or matched impedance backing, so the front surface of the transducer can move relative to the back surface. The advantages would be

easier and more mechanically stable alignment, higher capacity, and much higher breakdown fields. The disadvantage would be the far higher dc potentials required, a more complicated response characteristic, and still a very weak response relative to the piezoelectric transducer.

Suppose now a dc field E_0 is applied to an airgap transducer. The applied voltage is $V_0 = E_0 \ell$. The voltage change generated by a displacement u is

$$V = E_0 u \tag{15}$$

so the output of the transducer is proportional to the displacement of the acoustic wave.

B. The Piezoelectric Transducer

1. The Terminated Transducer

We make use of the Mason model of the transducer illustrated in Fig. 3[4] to show that its voltage output is

$$V_3 = \frac{h}{j\omega} (v_1 + v_2) \tag{16}$$

where v_2 is the input velocity on the right hand side of the transducer, $h = e/\varepsilon^s$, e is the piezelectric stress constant, and ε^s the constant strain dielectric constant.

When the transducer is terminated in a matched impedance Z_0 it follows that

$$v_2 = -v_1 e^{-j\beta\ell} \tag{17}$$

where ℓ is the transducer length, $\beta = \omega/V_0$ the wave propagation constant of the wave inside the transducer, and V_0

the wave velocity in the transducer material.

It therefore follows from Eqs. (8) and (17) that

$$V_3 = \frac{h}{j\omega}(1 - e^{-j\beta\ell})\frac{2Z_1}{Z_1 + Z_0}v^+ \tag{18}$$

At resonance $\beta\ell = \pi$ and $\omega = \omega_0$, so it follows that

$$V_3 = \frac{2h}{\pi V_0}\frac{2Z_1}{Z_0 + Z_1}v^+ \tag{19}$$

At low frequencies $\beta\ell = 0$, so it will be seen that

$$V_3 \to \frac{jh\ell}{V_0}\frac{2Z_1}{Z_0 + Z_1}v^+ \tag{20}$$

It follows that the piezoelectric transducer responds to the incident rf velocity of the wave rather than its displacement. Its voltage response at zero frequency to velocity is increased by a factor $\pi/2$ from that at resonance. However its power output is decreased (note the change in phase). The response to acoustic displacement u^+ is another matter. As $v^+ = j\omega u^+$, the response of the transducer to displacement varies linearly with frequency.

2. Rigid Backing

This situation may be of interest for transducer materials like PVF_2 which have a relatively low impedance and can be used with a rigid backing of brass or other relatively high impedance material.

In this case $v_2 = 0$ and

$$\frac{T_1}{v_1} = j \cot \beta \ell \tag{21}$$

so it follows that

$$V_3 = \frac{h}{j\omega} \frac{2Z_1}{Z_1 - jZ_0 \cot \beta \ell} \tag{22}$$

At resonance $\beta_a \ell = \pi/2$, and

$$V_3 = \frac{4h\ell}{j\pi V_0} v^+ \tag{23}$$

As $\omega \to 0$

$$V_3 \to \frac{2h\ell}{V_0} v^+ \tag{24}$$

We note that if $Z_1 = Z_0$ the matched transducers and rigid backed transducers have essentially the same response at the two major frequency ranges of interest. For the same resonant frequency, the rigidly backed transducer is half the length of the matched backed transducer.

3. Air Backed Structure

In this case the stress at the back of the transducer is zero, and we can write

$$v_1 = -v_2 \cos \beta \ell \tag{25}$$

This implies that

$$V_3 = -\frac{h}{j\omega} \frac{2Z_1}{(Z_1 + jZ_0 \tan \beta\ell) \cos \beta\ell} v^+ \qquad (26)$$

At resonance $(\beta\ell = \pi)$

$$V_3 = \frac{4v^+ h\ell}{j\pi V_0} \qquad (27)$$

As $\omega \to 0$ it follows that

$$V_3 \to \frac{jv^+ h\omega\ell^2}{V_0^2} \qquad (28)$$

Thus the response falls off at low frequencies. This is because the back of the transducer is free to move with the front surface, and so at low frequencies there tends to be no net applied strain. We therefore conclude that, as we might have expected, air backing is poor for use in broadband transducers.

VI. THE FIBER OPTIC TRANSDUCER

A new type of transducer which has generated considerable interest employs fiber optics. The basic idea behind this transducer is that when external pressure is applied to a fiber optic waveguide, there is a phase shift of the optical wave passing through the guide; this phase shift is proportional to the applied pressure. If the applied pressure is due to an incident acoustic wave, the acoustic wave signal will phase modulate the optical beam. The optical output can be mixed with a reference beam in an optical detector and so give rise to an

output from the mixer at the acoustic frequency.

The reason for the good sensitivity of this fiber optic transducer is that as the optical wavelength is of the order of 1 μm , a fiber 1 meter long is 10^6 wavelengths long. Hence a very small change in optical wave velocity translates into a relatively large change in phase shift of the optical wave. Typically the fibers are of the order of 100 μm diameter. In order not to exceed the breaking strain of the fiber, the fiber cannot be coiled into a coil much less than 5 mm radius, i.e. 1 cm diameter. Therefore a transducer of the order of 1 mm diameter is out of the question.[5] However, a transducer of the order of 1 cm diameter is possible by making a series of pancakes of several turns of the fiber placed one on top of the other. The fibers could be embedded in a tungsten epoxy matrix, which would be placed in contact with the structure being examined. If ℓ is the thickness of the active region, which is assumed to be terminated with a material of the same impedance, then the total phase shift through the fiber will be

$$\phi = Ak \int_0^{\ell} e^{-j\beta x}\, dx = \frac{Ak}{j\beta}\left(1 - e^{-j\beta\ell}\right) \tag{29}$$

where k is the propagation constant of the optical wave and A is a constant. This relation is similar in form to that of Eq. (18) for the piezoelectric transducer. Thus the magnitude of the phase response will vary as

$$|\phi| = Ak\ell \left|\frac{\sin \beta\ell/2}{\beta\ell/2}\right| \tag{30}$$

Therefore the 3 dB response of this transducer will be at a frequency f_0 where $\beta\ell = .9\pi/2$, i.e. where

$$f_0 \approx \frac{.45\ell}{V_0} \tag{31}$$

It follows that the area of the fiber pancakes limits the frequency and angular response in acoustic emission applications, and the total thickness of the pancake layers limits the frequency of the response because of the phase shift from layer to layer.

We can estimate the sensitivity of the fiber optic sensor by using the results of Budiansky et al. for application of hydrostatic pressure.[6] They show that the relative change in phase $\Delta\phi/\phi$ for quartz fiber is

$$\frac{\Delta\phi}{\phi} = 2.2 \times 10^{-12}\, p \tag{32}$$

Yariv[7] has shown that if the fiber is placed in a bridge circuit with the two fiber arms injected into a mixer, the signal to noise ratio of the system is

$$\frac{S}{N} = \frac{P\eta(\Delta\phi)^2}{4h\nu\Delta\nu} \tag{33}$$

where ν is the optical frequency, $\Delta\nu$ the required bandwidth, P the optical power of the laser, η the quantum efficiency of the detector and h Planck's constant. It follows that

$$\frac{S}{N} = 1.21 \times 10^{-24} \frac{P\eta p^2 \phi^2}{4h\nu\Delta\nu} \qquad (34)$$

However if the impedance of the material of the transducer is Z_0 , it follows that

$$\frac{S}{N} = 1.21 \times 10^{-24} \frac{P\eta Z_0^2 \phi^2}{h\nu\Delta\nu} \left(\frac{Z_1}{Z_0 + Z_1} \right)^2 \nu^{+2} \qquad (35)$$

VII. THE ACOUSTOELECTRIC TRANSDUCER

The acoustoelectric transducer makes use of the fact that when a piezoelectric semiconductor is excited by an acoustic wave, an acoustoelectric potential is set up along its length which is proportional to the square of the input signal. For this reason the device adds the square of the magnitudes of all entering signals and gives an output proportional to its length adding all signals entering its surface. Thus the device is phase insensitive and has a directivity which varies as $\cos \theta$, assuming electrodes are placed on its back and front surfaces.

Initially, therefore, it looks like a very attractive candidate for an acoustic emission sensor. But as it is a second order detector, its response is weak. Consequently, on the basis of very crudes estimates, we reject it as a sensor for this purpose.

VIII. PHASE ARRAY DETECTORS

One way out of the difficulty of the insensitivity of the acoustoelectric detector is to use an array of small transducers each connected to an individual high impedance amplifier. The outputs of these amplifiers are fed into individual square detectors and summed. Now the resultant device could be made of large area, and as sensitive as an individual piezoelectric transducer, without being phase sensitive.

A second possibility is to record the signal from each amplifier separately and process it appropriately. Suppose that the transducers were spaced a distance d and the signal arrived at an angle θ to normal to the array. Then if the emission signal is $F(t)$, a surface wave signal arriving along the substrate at the n^{th} transducer, at an angle θ to the normal of the plane of the array, is of the form

$$F(t - T - x_n \sin \theta/V_R)$$

at the n^{th} element, whose coordinates are $x_n, 0$, as illustrated in Fig. 4. By taking the time correlation of these signals with the signal from one element, say $x_n = 0$

$$G(t) = \int F(\tau - T)\, F(t + \tau - T\, x_n \sin \theta/V_R)\, d\tau \qquad (36)$$

we should observe a correlation peak at a time

$$t = x_n \sin \theta/V_R \qquad (37)$$

Hence we can find the angular position from which the signal arrived. In principle we need only two transducers for this purpose, but more would eliminate aliasing effects.

Alternatively we could take the Fourier transform of the signal and look at any particular frequency component ω . Then standard time delay or phase delay imaging techniques used on each frequency component would make it possible to locate the angular position of this component.

If the transducers are well spaced then the method of Eq. (36) tends to reduce to a triangulation technique and makes it possible to find the position of the source unequivocally.

IX. NUMERICAL CALCULATIONS

As an example for a PZT 5H transducer with a matched backing and a resonant frequenty of 2 MHz , ℓ = 1.1 mm , $h = 3/\varepsilon^S = 3.76 \times 10^9$ V/m , so $V_3 = 962v^+$. Now a 2N5558 low noise JFET has a response of 200×10^{-9} V/$\sqrt{\text{Hz}}$, so the noise over a 2 MHz bandwidth is 2.83×10^{-4} volts. Therefore, if we assume that for noise like emission sources we need a signal to noise ratio of 10 dB in order to observe emission unequivocally, we find that the minimum detectable velocity is $v = 9.1 \times 10^{-7}$ m/sec and the minimum detectable displacement is therefore $u = 1.4 \times 10^{-13} f$, where f is the operating frequency in MHz . If we take the diameter of the transducer to be 1 mm so the response falls off slightly more than 3 dB at 2 MHz in accordance with Eq. (5), we find that for PZT 5H , ($\varepsilon^S_{33}/\varepsilon_0 = 830$, $\varepsilon^T_{33}/\varepsilon_0 = 1700$) the capacity is between 6 and 12 pf . As the JFET has a capacity of the order of 2 pf , it will not load the transducer too severely.

The low capacity of the transducer militates agains the use

of a PVF_2 plastic piezoelectric material. Although the transmitting constant h is comparable to PZT, $\varepsilon^s/\varepsilon_0 \sim 4$, so a small transducer will be severely loaded by the external circuit.

A ZnO thin film transducer would suffer from the same difficulties, so the only realistic small diameter transducer that can be used is one made of PZT ceramic.

A similar calculation can be made for capacitor transducers. If we suppose that we use a transducer with 2 μm spacing, with very large applied field E_0 of 10^7 v/m corresponding to an applied voltage of 20V, it follows from Eq. (15) that the 2N558 JFET would give a 10 dB signal to noise ratio with a displacement $v = 9 \times 10^{-11}$m. It will be seen that a PZT transducer would have the same sensitivity at a frequency of 1.5 KHz. At higher frequencies the sensitivit of the PZT transducer increases linearly with frequency and so normally far exceeds that of the capacitive transducer.

For a fiber optic transducer with $P = 1$ mw, $\nu = 3 \times 10^8$ MHz, $\Delta\nu = 2$ MHz, and $\eta = 0.5$, we find that $\Delta\phi = 1.8 \times 10^{-4}$ for a 10 dB signal to noise ratio. Taking the impedance of the glass to be 15×10^6 kg/m^2-sec, we find that for a sensitivity equal to that of PZT $v = 9.1 \times 10^{-7}$ m/sec, $p = Z_0 v = 13.7$ kg/m2. Hence with $\Delta\phi/\phi = 2.2 \times 10^{-12}\, p$, $\Delta\phi/\phi = 2.7 \times 10^{-11}$ and $\phi = 6.6 \times 10^6$ radians, i.e. about 10^6 wavelengths. This corresponds to a fiber length of approximately 1 meter. Such a fiber could be coiled up into approximately 30 turns of 1 cm diameter in the form of several pancake layers, as already described.

X. CONCLUSIONS

A study has been made of the merits of different types of broadband acoustic transducers for observing acoustic emission in the frequency range from 100 KHz to 2 MHz . The criteria for good frequency response to Rayleigh waves and good frequency response to longitudinal waves have been derived. We conclude that a transducer of the order of 1 mm diameter is required.

The sensitivities for capacitor transducers, piezoelectric transducers, and fiber optic transducers have been derived. It has been shown that piezoelectric transducers which are velocity sensitive are several orders of magnitude more sensitive than capacitor transducers in the frequency range of interest. Capacitor sensors are, at best, only suitable for calibration purposes. PZT ceramic transducers terminated in a matched backing are the best choice because of the high dielectric constant of the material, which implies a transducer with a reasonable impedance at the frequencies of interest. ZnO thin film integrated circuit transducers are not a good choice because the FET used has too high a gate capacity, the ZnO layer is likely to be too thin for good sensitivity, and it is difficult but not impossible to provide a matched backing layer. PVF_2 transducers are not suitable because they have too low a capacity, so they tend to be too heavily loaded by the input amplifier at the frequencies of interest.

The fiber optic transducer has been analyzed. It is shown that for sensitivity comparable to a PZT transducer,

approximately 1 meter length must be employed. The fiber must be coiled in the form of several pancake spiral layers embedded in a tungsten epoxy matrix. But the minimum diameter can only be of the order of 1 cm thus making the angular response unsuitable for this application. The frequency response is limited also by the thickness of the multiple layer system because of the phase change of the acoustic waves passing through these layers. Thus with a 1 cm diameter the frequency response would drop off at approximately 200 KHz . By coiling the fiber to a diameter of 2 - 3 mm, the working frequency could be raised to 1 MHz , but at the risk of a very short life.[8] The development of smaller diameter single mode fibers could change this conclusion and make it possible to use fibers at higher frequencies. At all events the fiber optic sensor is an attractive candidate for lower frequency operation because it should not suffer from electromagnetic interference.

Acknowledgement

The main part of this work was supported by the Advanced Research Projects Agency of the Department of Defense under Contract No. MDA903-80C-0505 with the University of Michigan. It was completed at Stanford with support by the Air Force Office of Scientific Research under Contract No. F49620-79C-0217.

References

1. Y. Pao, "Theory of Acoustic Emission," Elastic Wave and Nondestructive Testing of Materials, AMD 28, edited by Y.H. Pao, ASME, 1978.
2. G.S. Kino and C.S. DeSilets, "The Design of Slotted Transducer Arrays with Matched Backing," Ultrasonic Imaging, vol. 1, p. 189, 1979.
3. G.F. Miller and H. Pursey, "The Field and Radiation Impedance of Mechanical Radiations on the Free Surface of a Semi-Infinite Isotropic Solid," Proc. Roy. Soc. London, vol. 223, p. 521, 1954.
4. B.A. Auld, Acoustic Fields and Waves in Solids, vol. 1, Wiley, 1973.
5. G.S. Kino and R.M. Thomson, "Detection and Evaluation of Small Flaws in Optical Fibers," MRC Report, DARPA Materials Research Council, July 1980.
6. B. Budiansky, D. Drucker, G.S. Kino, and J. Rice, "The Pressure Sensitivity of a Clad Optical Fiber," Appl. Optics, vol. 18, p. 4085, 1979.
7. A. Yariv and H.V. Winsor, Proposal for Detection of Magnetic Fields Through Magnetostructive Perturbation of Optical Fibers, Optics Lett., vol. 5, p. 87, 1980.
8. T. Yamanishi, K. Yoshimura, S. Seuuki, S. Seikai, and N. Ochida, "Modified Silicone as a New Type of Primary Coat for Optical Fibre," Electr. Lett., vol. 16, no. 3, p. 100, 1980.

Figure Captions

1. Illustration of a surface wave propagating at an angle ϕ to the x axis.
2. Illustration of a longitudinal wave incident on the surface at an angle θ.
3. Schematic of a transducer with velocities v_1, v_2 on its two sides, excited by a wave of velocity amplitude v^+ incident on the surface of the substrate.
4. Illustration of an array receiving a signal from a distant source.

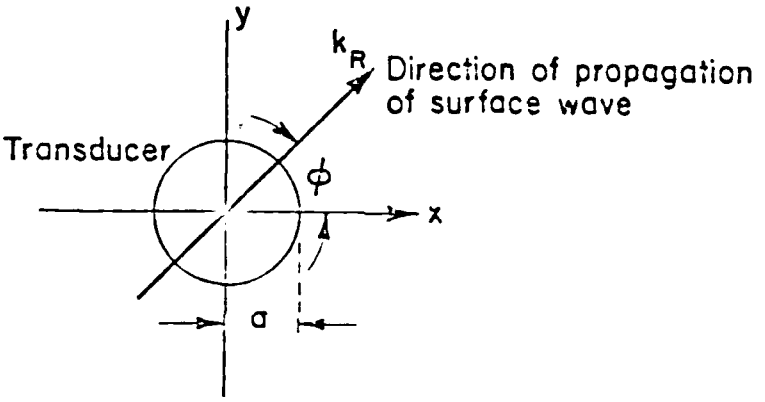
y
k_R
Direction of propagation
of surface wave
Transducer
ϕ
x
a

Figure 1.

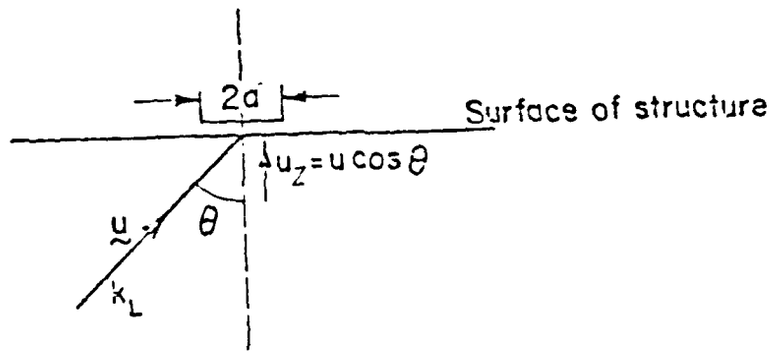
2a
Surface of structure
$u_z = u \cos\theta$
$\underset{\sim}{u}$
θ
k_L

Figure 2.

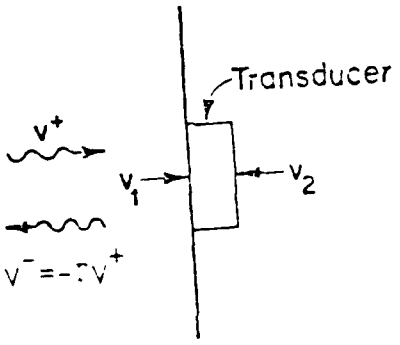

Figure 3.

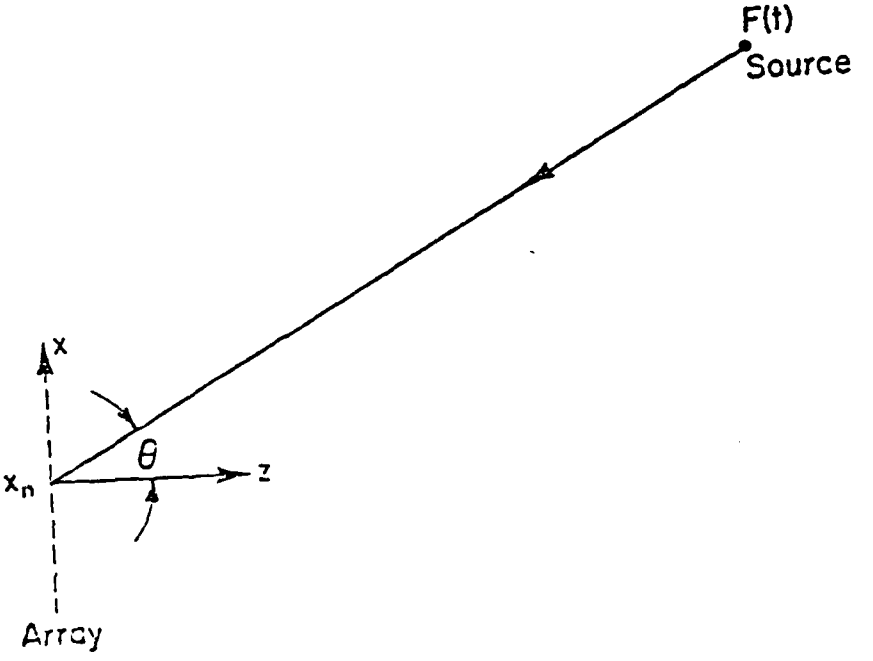

Figure 4.

DISTRIBUTION LIST
Report No. NADC-81087-60

	Copies
Naval Air Development Center (60633)	20
Naval Air Development Center (8131)	3
Defense Advanced Research Projects Agency TIO/ADMIN	3
Defense Documentation Center	12
Southwest Research Institute-NTIAC	1
Battelle, Pacific Northwest Laboratories	21